MUHAMMAD SAGIR MUHAMMAD

COMPARATIVE STUDY OF GFRP AND STEEL BARS IN RC MEMBERS

NEU 2019

COMPARATIVE STUDY OF GLASS FIBER REINFORCED POLYMER (GFRP) AND STEEL BARS IN REINFORCED CONCRETE (RC) MEMBERS

A THESIS SUBMITTED TO THE GRADUATE SCHOOL OF APPLIED SCIENCES OF NEAR EAST UNIVERSITY

By
MUHAMMAD SAGIR MUHAMMAD

In Partial Fulfilment of the Requirements for the Degree of Masters in Science in Civil Engineering

NICOSIA, 2019

COMPARATIVE STUDY OF GLASS FIBER REINFORCED POLYMER (GFRP) AND STEEL BARS IN REINFORCED CONCRETE (RC) MEMBERS

A THESIS SUBMITTED TO THE GRADUATE SCHOOL OF APPLIED SCIENCES
OF
NEAR EAST UNIVERSITY

By
MUHAMMAD SAGIR MUHAMMAD

In Partial Fulfilment of the Requirements for the Degree of Masters in Science
in
Civil Engineering

NICOSIA, 2019

I hereby declare that all information in this document has been obtained and presented in accordance with academic rules and ethical conduct. I also declare that, as required by these rules and conduct, I have fully cited and referenced all material and results to this work.

Name, Last Name: Muhammad Sagir Muhammad

Signature:

Date: 15/03/19

Dedicated to my parents and siblings…

ACKNOWLEDGEMENTS

My immense gratitude goes to my hard working supervisor Assoc. Prof. Dr. Rifat Reşatoğlu, for assisting and guiding me from the beginning until the ending of this research work. His dedication, motivation and encouragement towards the success of this work was an interesting experience. My gratitude also goes to Prof. Dr. Kabir Sadeghi for his help and guidance towards the completion this thesis work.

My gratitude goes to Mr. Menteş Haskasap, Mr. Yiğit Gūrdal, and the foremen at Near East University mosque construction site for their immense help.

I would also like to express my appreciation to chairman Chambers of Civil Engineers Mr. Gūrkan Yağcioğlu for giving me the approval to perform some of the experimental works in their laboratory. My gratitude also goes to Mr. Mustafa Turk and Enver Toker for their support in carry out the experiments in the Laboratory.

I would also use this opportunity to deeply appreciate my parents for their financial support and prayers throughout my educational career.

ABSTRACT

Corrosion is one of the essential factors that affects serviceability and performance of reinforced concrete structures more importantly in the coastal areas. It results to early degradation and damage. Glass fibre reinforced polymer (GFRP) bar is one of the promising alternative material to conventional steel bar that is proven to solve the corrosion problem.

This thesis aims to investigate the behavior of steel and GFRP bars in concrete with regards to bonding and flexure. The flexural behavior of reinforced concrete beams under experimental work and finite element analysis (ABAQUS) is also compared to check the feasibility of GFRP bar as reinforcement material. Six beams were prepared each having dimensions 750x150x150mm and four point bending test was performed until failure. The beams were having 1%, 1.4% and 2.1% reinforcement ratios using each of the reinforcement bar. The parameters to check includes the ultimate load capacity, flexural strength, mode of failure, crack patterns, crack width and the ultimate bond strength. The pull-out test showed adhesion between GFRP bars and concrete was perfect as the failure experienced was concrete splitting unlike steel bar which slipped and pulled out of the concrete. It was observed that the flexural strength and ultimate load capacity of group 2 beams (GFRP) was lower than that of group 1 beams (steel). The failure modes experienced in both group 1 group 2 beams were shear failure which was due to the limited span length. Group 2 beams experienced higher crack width than group1 beams due to the brittle nature of the GFRP bar. There was close agreement between the experimental and FEA results. The cost of GFRP bar is higher than steel bar but still regarded as a good alternative due to its non-maintenance and non-corrosive benefit.

Keywords: ABAQUS; Glass fibre reinforced polymer (GFRP) bar; finite element analysis; flexural strength; ultimate bond strength

ÖZET

Korozyon, kıyı bölgelerinde betonarme yapıların kullanılabilirliğini ve performansını etkileyen önemli etkenlerden biridir. Erken aşınma ve hasara yol açarlar. Geleneksel betonarme çeliğine alternatif malzemelerden olan Cam lif takviyeli polimer çubukların korozyon problemlerini çözdükleri kanıtlanmıştır.

Bu tezdeki asıl amaç, betonarme çelik ve GFRP çubukların beton içerisindeki aderans ve eğilme davranışını araştırmaktır. Bunun için deneysel çalışmalar yardımı ile betonarme kirişlerdeki eğilme davranışı ve sonlu elemanlar analizi (ABAQUS) ile GFRP çubuklarının donatı çeliği olarak kullanılabilirliğini kontrol etmek için karşılaştırma yapılmıştır. Her biri 750x150x150mm boyutlarında altı kiriş numunesi hazırlanmış ve kırılma noktasına kadar dört noktadan eğilme testi yapılmıştır. Kirişlerde, 1%, 1.4% ve 2.1% donatı oranına sahip çubuklar kullanılmıştır. Kontrol edilen parametreler, son taşıma yükü, eğilme dayanımı, kırılma noktası, çatlama biçimi, çatlak genişlikleri ve aderans dayanımıdır. Çıkarma testinde, betondan kayarak çıkarılan çelik çubuğun aksine GFRP çubuk ile beton arasındaki aderansın, betonun parçalanması nedeniyle mükemmel olduğunu göstermiştir. Grup 2 kirişlerin (GFRP) eğilme dayanımı ve son yük taşıma kapasitesi, grup 1 kirişlerden (çelik) daha düşük olduğu görülmüştür. Grup 1 ve grup 2 kirişlerinde gözlemlenen kırılma noktaları sınırlı açıklık uzunluğuna bağlı kesme (kayma) kırılmasından ötürüdür. GFRP çubuğunun gevrek olması nedeniyle, grup 2 kirişlerinin, grup 1 kirişlerine göre daha yüksek çatlak genişliğinde olduğu görülmüştür. Deneysel ve FEA sonuçları arasında yakın bir uyuşum olduğu görülmüştür. GFRP çubuğunun maliyeti, çelik çubuğa göre daha yüksektir, ancak bakım gerektirmeyen ve korozif olmayan özellikleri nedeniyle, alternatif malzeme olarak görülmektedir.

Anahtar kelimeler: ABAQUS; Cam lif takviyeli polimer (GFRP) çubuk; sonlu elemanlar analizi; eğilme dayanımı; aderans dayanımı

TABLE OF CONTENTS

ACKNOWLEDGEMENTS ii

ABSTRACT iii

ÖZET ………. iv

TABLE OF CONTENTS v

LIST OF TABLES.. x

LIST OF FIGURES.. xi

LIST OF SYMBOLS.. xiv

CHAPTER 1: INTRODUCTION

1.1 Background.. 1

1.2 Statement of Problem 3

1.3 Aims of the Thesis 5

1.4 Scope and Limitations 6

1.5 Organization of Thesis.. 6

CHAPTER 2: FIBRE REINFORCED POLYMER (FRP) MATERIAL IN CIVIL ENGINEERING

2.1 General... 8

2.2 History of Fibre Reinforced Polymer (FRP) Reinforcement.......................... 8

2.3 Fibre Reinforced Polymer (FRP) Bar 9

2.4 Manufacturing Process 9

2.5 Types of Fibre Reinforced Polymer (FRP) Bar 10

2.6 Advantages and Disadvantages of FRP Bars 11

2.6.1 Advantages 11
2.6.2 Disadvantages 12
2.7 Fibre Reinforced Polymer (FRP) Properties 12
2.7.1 Mechanical properties 12
2.7.1.1 Compressive behavior 13
2.7.1.2 Tensile behavior 13
2.7.1.3 Shear behavior 15
2.7.1.4 Bond behavior 15
2.7.2 Physical properties 16
2.7.2.1 Coefficient of thermal expansion 16
2.7.2.2 Density 17
2.7.2.3 Effects of fire and high temperature 17
2.7.2.4 Thermal conductivity 17
2.7.3 Long-term behaviours 18
2.7.3.1 Creep rupture 18
2.7.3.2 Fatigue 18
2.7.3.3 Durability 19
2.8 Glass Fibre Reinforced Polymer (GFRP) Bar 19
2.9 GFRP Applications in Civil Engineering 21
2.9.1 Parking garages 22
2.9.2 Bridges 22
2.9.3 Rail 24
2.9.4 Airport runways 24
2.9.5 Medical and information technology 24
2.9.6 Seawalls 25
2.9.7 Unique structures 26

2.9.8 Precast 27

2.10 Previous Experimental Studies 27

CHAPTER 3: FAILURES IN SIMPLE BEAM AND DESIGN GUIDELINES

3.1 Introduction 31

3.2 Flexural Failure 31

3.3 Diagonal Tension Failure 32

3.4 Shear Compression Failure 33

3.4 Design Philosophy 33

3.4.1 Flexure limit state 34

3.4.2 Serviceability limit state 37

3.4.2.1 Cracking 38

CHAPTER 4: EXPERIMENTAL STUDY

4.1 General 39

4.2 Materials 39

4.2.1 Concrete 39

4.2.2 Steel bars 39

4.2.3 Glass fibre reinforced polymer (GFRP) bars 39

4.3 Equipment 40

4.3.1 Automatic compression machine 40

4.3.2 Universal testing machine 40

4.3.3 Pull-out test apparatus 41

4.3.4 Flexural testing machine 41

4.4 Test Procedures 42

4.4.1 Testing reinforcing bars 42
4.4.2 Testing concrete cube strength.. 43
4.4.3 Testing bonding behaviour.. 44
4.4.4 Testing flexural behaviour 45
4.4.4.1 Description of beam specimens 45
4.4.4.2 Geometry of the beam specimens 46
4.4.4.3 Preparation of beams.. 47
4.4.4.4 Four point bending test.. 49

CHAPTER 5: FINITE ELEMENT ANALYSIS (ABAQUS)

5.1 General.. 51
5.2 Modelling of beam specimens.. 51
5.2.1 Concrete 51
5.2.2 Reinforcement.. 52
5.3 Material Properties 53
5.3.1 Concrete 53
5.3.2 Steel bar.. 53
5.3.3 GFRP bar.. 54
5.4 Loading and Boundary Conditions.. 54

CHAPTER 6: RESULTS AND DISCUSSIONS

6.1 General.. 55
6.2 Tensile Behaviour.. 55
6.2 Bond Behaviour.. 57
6.3 Flexural Behaviour 60

6.3.1 Ultimate load capacity 60

6.3.2 Flexural strength 62

6.3.3 Failure mode 62

6.3.4 Crack width 65

6.3.5 Summary of flexural behaviour results 66

6.4 Finite Element Analysis Results 67

6.4.1 Ultimate load capacity and failure modes 67

6.5 Experimental and FEA Results Comparison 70

6.6 Cost Comparison 72

CHAPTER 7: CONCLUSIONS AND RECOMMENDATIONS 75

REFERENCES 77

APPENDICES

Appendix 1: Graphical results of the compression, tensile, flexural and pull-out tests 84

Appendix 2: Stress strain relationship of concrete parameters 90

Appendix 3: Price list of Liana glass fibre reinforced polymer (GFRP) bar 92

LIST OF TABLES

Table 2.1: Tensile properties of steel and FRP bars 15
Table 2.2: Coefficient of thermal expansion of steel bar and FRP bars 16
Table 2.3: Density of steel bar and FRP bars 17
Table 2.4: Types of glass fibre 20
Table 2.5: Chemical composition of different types of GFRP 21
Table 3.1: Environmental factor of reduction under different condition of exposure 34
Table 4.2: Concrete strength of cubes 44
Table 4.3: Beam details 46
Table 4.4: Beam design calculation parameters 47
Table 5.1: Material properties of concrete 53
Table 5.2: Material properties of steel bar used 54
Table 5.2: Material properties of GFRP bar used 54
Table 6.1: Mechanical properties of steel bars 55
Table 6.2: Mechanical properties of GFRP bars 56
Table 6.3: Summary of pull-out test results 58
Table 6.4: Flexural strength of beam specimens 62
Table 6.5: Crack width of beam specimens 66
Table 6.6: Experimental flexural test results 66
Table 6.7: Summary of FEA flexural results 67
Table 6.8: Cost of reinforcement bars 73
Table 6.9: Total cost of reinforcement cage of specimens 74

LIST OF FIGURES

Figure 1.1: Leo Frigo Memorial Bridge failure ... 2
Figure 1.2: Damage due to corrosion of an old building in Gazimagusa, North Cyprus ... 2
Figure 1.3: Total number of structures in TRNC over the years ... 5
Figure 2.1: Component of an FRP bar ... 9
Figure 2.2: Pultrusion process ... 10
Figure 2.3: Samples of FRP bar ... 11
Figure 2.4: Stress strain curve of reinforcement bars ... 13
Figure 2.5: Types of bar surface ... 20
Figure 2.6: La Chanceliere Parking Garage in Quebec, Canada ... 22
Figure 2.7: Bridge Deck in Morristown – Vermont, USA ... 23
Figure 2.8: Sierrita de la Cruz Creek Bridge, Potter County, Texas ... 23
Figure 2.9: GFRP Bridge Deck, Cookshire-Eaton, Quebec ... 23
Figure 2.10: GFRP as railway plinths ... 24
Figure 2.11: MRI room in Lincoln General Hospital, NE, USA ... 25
Figure 2.12: Trauma Centre in York Hospital, USA ... 25
Figure 2.13: Seawall restoration in Palm Beach Florida, USA ... 26
Figure 2.14: Seawall of Lyles residence in California, USA ... 26
Figure 2.15: Pyramid shaped winery in British Columbia ... 26
Figure 2.16: Hindu temple design with service life of 1000 years ... 27
Figure 2.17: Culvert bridge in City of Rolla, Phelps County, Missouri ... 27
Figure 3.1: Illustration of flexural failure ... 31
Figure 3.2: Diagonal tension failure of concrete beam ... 32
Figure 3.3: Illustration of shear compression failure ... 33
Figure 3.4: Reduction factor of strength (American Concrete Institute, 2015) ... 37
Figure 4.1: Compression testing machine (UTC-4320) ... 40
Figure 4.2: Universal testing machine (UTM-4000) ... 40
Figure 4.3: Pull-out apparatus ... 41
Figure 4.4: Automatic flexural testing machine (UTC-4620) ... 41
Figure 4.5: GFRP bar specimen ... 42

Figure 4.6: Schematic diagram of GFRP bar specimen ... 43
Figure 4.7: Concrete cube moulds and casted specimens ... 43
Figure 4.8: Preparation of pull-out specimens ... 45
Figure 4.9: Details and dimensions of all group 1&2 beams ... 47
Figure 4.10: Preparation of beam moulds before concrete casting ... 48
Figure 4.11: Casting of beam specimens ... 48
Figure 4.12: Curing of beam specimens ... 49
Figure 4.13: Diagram of loading arrangement of beams in flexural machine ... 49
Figure 4.14: Loading setup of beams ... 50
Figure 5.1: Sample of beam model used ... 52
Figure 5.2: Sample of reinforcement cage embedded in the RC beam ... 52
Figure 6.1: Slippage between the GFRP bar and hardened polyester adhesive ... 57
Figure 6.2: Slippage between the hardened epoxy and steel tube ... 57
Figure 6.3: Comparison of maximum bond strength of pull-out specimens ... 58
Figure 6.4: S1 & S2 specimen failure mode ... 59
Figure 6.5: G1 specimen failure ... 59
Figure 6.6: G2 Specimen Failure ... 59
Figure 6.7: Ultimate load capacity comparison of G1-BM1 & G2-BM1 beam ... 60
Figure 6.8: Ultimate load capacity comparison of G1-BM2 & G2-BM2 beam ... 61
Figure 6.9: Ultimate load capacity comparison of G1-BM3 & G2-BM3 beam ... 61
Figure 6.10: Failure mode in beam G1-BM1 ... 63
Figure 6.11: Failure mode in beam G2-BM1 ... 63
Figure 6.12: Failure mode in beam G1-BM2 ... 64
Figure 6.13: Failure mode in beam G2-BM2 ... 64
Figure 6.14: Failure mode in beam G1-BM3 ... 65
Figure 6.15: Failure mode in beam G2-BM3 ... 65
Figure 6.16: FEA failure mode of G1-BM1 ... 68
Figure 6.17: FEA failure mode of G2-BM1 ... 68
Figure 6.18: FEA failure mode of G1-BM2 ... 69
Figure 6.19: FEA failure mode of G2-BM2 ... 69
Figure 6.20: FEA failure mode of G1-BM3 ... 70
Figure 6.21: FEA failure mode of G1-BM3 ... 70

Figure 6.22: Comparison of FEA and experimental result for G1-BM1 & G2-BM1 71
Figure 6.23: Comparison of FEA and experimental result for G1-BM2 & G2-BM2 71
Figure 6.24: Comparison of FEA and experimental result for G1-BM3 & G2-BM3 72

LIST OF SYMBOLS

$\boldsymbol{a}$:	Depth of equivalent rectangular stress block (mm)
$\boldsymbol{A_f}$:	Area of fibre reinforced (FRP) bar (mm^2)
$\boldsymbol{b}$:	Width of rectangular cross-section (mm)
$\boldsymbol{c}$:	Distance from extreme compression fibre to the neutral axis
$\boldsymbol{D}$:	Diameter of bar (mm)
$\boldsymbol{d}$:	Distance from extreme compression fibre to centroid of tension bar (mm)
$\boldsymbol{d_c}$:	Thickness of concrete cover (mm)
$\boldsymbol{E_f}$:	Modulus of elasticity of FRP bar (MPa)
$\boldsymbol{F}$:	Maximum applied force (kN)
$\boldsymbol{f'_c}$:	Compressive strength of concrete (MPa)
$\boldsymbol{f_f}$:	Stress of FRP bar in tension (MPa)
$\boldsymbol{f_{cf}}$:	Flexural strength of beam (MPa)
$\boldsymbol{f_{fu}}$:	Design tensile strength of FRP (MPa)
$\boldsymbol{k_b}$:	Bond-dependent coefficient
$\boldsymbol{L}$:	Embedded length (mm)
$\boldsymbol{M_n}$:	Nominal moment capacity (N-mm)
$\boldsymbol{P_{max}}$:	Maximum applied load
$\boldsymbol{s}$:	Stirrup spacing (mm)
$\boldsymbol{w}$:	Crack width (mm)
$\boldsymbol{\beta_1}$:	Factor taken as 0.85
$\boldsymbol{\varepsilon_{cu}}$:	Ultimate strain in concrete
$\boldsymbol{\rho_f}$:	FRP bar reinforcement ratio
$\boldsymbol{\rho_{fb}}$:	FRP bar reinforcement ratio producing balanced strain conditions
$\boldsymbol{\tau_b}$:	Ultimate bond strength
$\boldsymbol{\varphi}$:	Strength reduction factor

CHAPTER 1

INTRODUCTION

1.1 Background

Concrete is a known composite material consisting of cement, aggregates and water, it is weak in tension but strong in compression. Use of steel assist in resisting tensile forces in concrete elements. There has always been an interest for a material having both extreme strength and ductility. Strength gives a member the ability to carry load safely while ductility avoids sudden failure. "Mild steel have been the best option for years providing strength and ductility of simple, homogeneous materials is incompatible, although metals (e.g., mild steel) have been the best option" (Kheni et al., 2016). Steel bars being the conventional material for reinforcing structural concrete, they last for years without any physical sign of damage if corrosion attack is prevented. But corrosion attack is impossible to prevent in structures open to certain environments like de-icing salts in bridge, marine structures, parking structures, bridge decks, highway under extreme environments, etc. When temperature and chlorides are combined with moisture, the speed of corrosion of steel bar is increased leading to deterioration and finally affect the serviceability of the structure.

In general, due to the corrosion attack to steel reinforcement it was estimated that up to 15% of all bridges are deficient structurally. In United Sates, it was estimated that an approximate amount of $8.3 billion is associated to annual direct cost of repair and maintenance of these structures (Salh, 2014). In Canada, the average cost of repair and maintenance of reinforced concrete structures in a year amount to almost $74 billion and in Europe, this amount is estimated to be around $3 billion per annum (Balendran et al., 2002). Figure 1.1 shows a bridge in Wisconsin which was built in 1980 which collapsed in 2013 as a result of corrosion of underground steel supporting the piers, the repair cost amount to $18-$20 million and the closure of the bridge for about three months leads to loss of about $14.5 million (NACE International, 2013). Figure 1.2 also shows a pedestrian bridge built in 1995 that failed in 2002 due to corrosion of steel support that occurs as a result of calcium chloride (a highly corrosive compound), the incident leads to injury to about 100 individuals (NACE

International, 2000). Figure 1.3 shows an incident of an old building in Gazimagusa, North Cyprus where there is cracks and spalling of concrete, this happens because the aggregates used in concrete where from the sea and possibly seawater was used in the mix (Naimi & Celikag, 2014).

Several methods are employed to solve the problem of corrosion and to increase service life of RC structures, they include metallic coating, protective coating, corrosion inhibitors, corrosion resistance alloys, anodic and cathodic protection, use of corrosion resistance composites and stainless steel. But most of the aforementioned solutions have less success rate or are very expensive (Salh, 2014). Use of fibre reinforced polymer bar as internal reinforcement in concrete elements is one of the preferred solution adopted around the world due to its positive results over the years.

Figure 1.1: Leo Frigo Memorial Bridge failure (NACE International, 2013)

Figure 1.2: Damage due to corrosion of an old building in Gazimagusa, North Cyprus (Naimi & Celikag, 2014)

Fibre reinforced polymer (FRP) composite are materials manufactured from fibres and resins. GFRP (glass), AFRP (aramid) and CFRP (carbon) are the commonly known use of FRPs regarding applications in civil engineering (Sonnenschein et al., 2016). These materials are now used in prestressed and reinforced concrete elements for reinforcement, repair and strengthening of already built structures and manufacture of ground anchors (Worner, 2015). Lack of enough information and design specification limit the extensive use of them as reinforcements. Fibre reinforced polymer (FRP) bars were recently introduced in the market as substitute of steel for internal reinforcement in concrete structures exposed to environments likely to cause corrosion. The use of fibre reinforced polymer (FRP) is regarded as one of the preferred solution today by a great number of countries as an internal reinforcement for concrete elements. However, some countries have started to make use FRP bars as reinforcements in their concrete structures.

Fibre reinforced polymer (FRP) bar is insusceptible to corrosion and chloride attack because it is a non-metallic material. Durability defects and decrease in service life of structures experienced due to use steel bar will be eliminated with FRP bar. FRP bar is cost effective due to better tensile strength to weight ratio when compared to typical steel bar. FRP bars main benefit over steel bars is the tensile strength which is three times higher, lower density, resistance to fatigue, chemical attack and corrosion and long term durability (Devi, 2015).

1.2 Statement of Problem

Reinforced concrete is the most prevalent composite material used in construction in the world and particularly in Turkish Republic of Northern Cyprus (TRNC). “From late 1970 till today the reinforced concrete structures are dominating building construction in North Cyprus” (Naimi & Celikag, 2014). Over the years the number of building has significantly rise. The Figure 1.3 shows the number of structures from the year 1993 to 2016, this implies there is need for reconsideration in materials and methods of construction such as use of sustainable materials. TRNC being an island has a lot of structure on the coast which are open to seawater that causes corrosion and also when aggregates extracted from sea is used in concrete mix.

Steel bar being the conventional material for construction have certain disadvantages when compared with FRP bar (such as corrosion) which will later be discussed in Chapter 2, these disadvantages renders it not 100% perfect. There are several methods of controlling corrosion such as using epoxy coated steel bar, but it was found out that using this method service life is extended by 5 years which is not cost effective (Michael, 2002). Cathodic protection being one of the effective methods of controlling corrosion requires occasional maintenance (Rob et al., 2012). Old infrastructures and the inflating costs of maintaining them is not only a North Cyprus issue, but a global problem. The corrosion problem is associated with maintenance which increases the life cycle cost of a structure.

Steel bar is heavier than FRP bar, therefore use of steel in RC structures significantly increase the overall weight of the structure and it is important to keep the weight of structures to a minimum. This implies there is need for use of lighter construction materials which will be of benefit for the overall performance of the structures.

In 1991, in Kumköy and Gaziveren, Güzelyurt, North Cyprus stones used for aggregates in construction works were collected from the seaside which cheaper than blowing up part of the mountains to get the aggregates, these stone contains salt deposits which needs to be washed but were not because they will eventually leads to corrosion easily. These aggregates were used for construction until 1993 when the government close the quarry and regarded the stones harmful for construction (Gökçekuş, 1994).

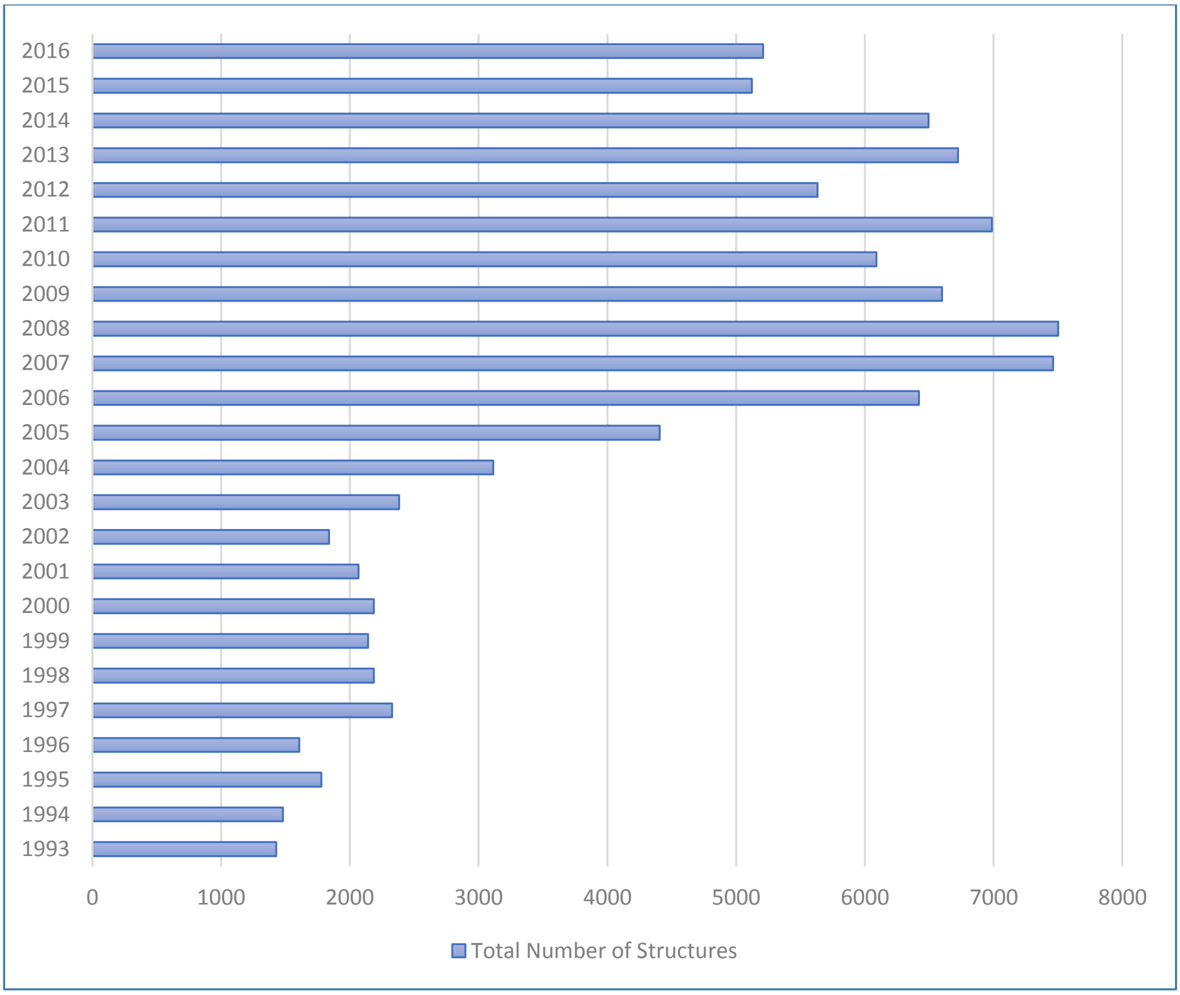

Figure 1.3: Total number of structures in TRNC over the years (State Planning Organization, 2016)

1.3 Aims of the Thesis

There is need for an alternative sustainable material to replace traditional steel bar. FRP bars being a good option solves problems associated to steel bars. These materials are guaranteed to be corrosion resistant and reduces the lifecycle cost of concrete structures. One of the aim is to identify and study the different types of FRP materials and compare their physical and mechanical properties to the conventional steel bar.

The main aim of this thesis is to compare the flexural behavior of steel and GFRP reinforced concrete element experimentally and using finite element analysis (FEA) done by ABAQUS. The bond behavior will be investigated using pull-out test and the reinforcement materials will also be tested to determine the mechanical properties and validate the specifications given by the manufacturer. The flexural test will be in two groups, one group will be reinforced with GFRP bar and other group will be reinforced with steel bar. The beams will be subjected to flexural test until failure to determine the ultimate load capacity, failure mode, crack pattern and crack width attributed to each of the beam. Cost comparison will also be done to check how effective GFRP bars are if used as reinforcing materials in concrete members.

1.4 Scope and Limitations

The study focuses on the evaluation of glass fibre reinforced polymer (GFRP) bar and also identifying its competency as a tensile reinforcing material in reinforced concrete members. The behaviour of the GFRP reinforced concrete members is also compared to steel reinforced concrete members having same dimensions and reinforcement ratios. Finite element analysis (FEA) using ABAQUS software will be done also to compare the results with the experimental results.

The limitations in this study are; (i) limited clear height of tensile machine making it unable to conform to the length proposed in the ASTM standard, (ii) short beam span which will affect the flexural behaviour result

1.5 Organization of Thesis

The thesis is made up of 7 chapters:

Chapter 1: This chapter gives the general information regarding reinforced concrete and the problems associated to it in North Cyprus. The aims and objectives, scope and limitations of the research is also stated.

Chapter 2: This chapter gives the in depth information regarding fibre reinforced polymer (FRP) bars stating their physical and mechanical properties, applications in civil engineering. Previous experimental studies done on GFRP bars will also be stated.

Chapter 3: This chapter will state the different failures attributed to simple beams and the design guidelines of ACI440 1.R-15 will be summarized which is used in designing the GFRP beams.

Chapter 4: This chapter present the experimental procedure that will be carried out on the reinforcement materials and the reinforced beams.

Chapter 5: This chapter gives information regarding finite element analysis using ABAQUS software.

Chapter 6: This chapter presents the experimental and the analytical results for comparison.

Chapter 7: This chapter presents the conclusions and recommendations for future actions to be taken.

CHAPTER 2

FIBRE RENIFORCED POLYMER (FRP) MATERIAL IN CIVIL ENGINEERING

2.1 General

This chapter will present the history of fibre reinforced polymer (FRP) materials as reinforcing materials in civil engineering. It will also present the types of FRP bars and give in depth information regarding their physical and mechanical properties and compare them with conventional steel bar. The advantages and disadvantages of using FRP bars will also be stated. Previous studies carried out on GFRP will summarized and presented.

2.2 History of Fibre Reinforced Polymer (FRP) Reinforcement

In the 1900's, scientists discovered synthetic resins (plastics) which surpass natural resins and materials, but plastics alone cannot yield the needed strength for some engineering requirements of advancing technology. In 1935, the first glass fibre combined with modern synthetic resins was discovered by Owens Corning (Mateenbar.com, 2018). The thought of bringing different materials together to invent a composite material is a something new but can be traced back when straw was used as reinforcement in mud in ancient Egypt to make a durable composite material, FRP is a modern and modified model of that former idea (Salh, 2014). FRP bars was known but not regarded as a good solution and not available commercially till late 1970s (American Concrete Institute, 2015).

The FRP industry began at the time of World War II, which leads to usage and improvement of FRPs. As the war ends, the industry was in full swing producing planes, cars and planes making the most use of this high strength, lightweight material (Mateenbar, 2018).

In 1980s, there was a demand for non-metallic material for reinforcement for certain advanced technology. High demand for this material was for buildings to house MRI medical equipment, and it was regarded as the accepted material for such type of construction. In mid 1990s, the total applications of FRP reinforcement in Japan in both private and commercial projects was more than 100 (Machida & Uomoto, 1997). China in the 2000s became the country with highest number of construction using FRP reinforcement ranging from underground work to bridge decks (American Concrete Institute, 2015). In 1986, the application of FRP reinforcement started in Europe, a prestressed highway bridge was constructed using FRP as reinforcement (American Concrete Institute, 2015).

2.3 Fibre Reinforced Polymer (FRP) Bar

Fibre reinforced polymer (FRP) bars are reinforcement materials that consist of continuous fibres held together in a polymeric resin matrix. This combination give rise to the physical and mechanical properties required for several filed of applications.

The fibres used in making FRP bars are continuous fibres, they have high strength coupled with high stiffness and lightweight as well. Fibres are responsible for the required strength. Carbon, glass, aramid and basalt are the common types of fibres used in making FRP bars

The polymeric matrix function is holding fibres together and prevent damage to the surface when is being manufactured, transported or in use and also throughout the service life of the bars. Another important role played by the matrix regarding strength of the bars is transferring stresses to the fibres via the matrix. The compatibility of fibres and the resin matrix should be good in terms of chemical and thermal properties. Some types of resins are polyester, epoxy and vinyl esters.

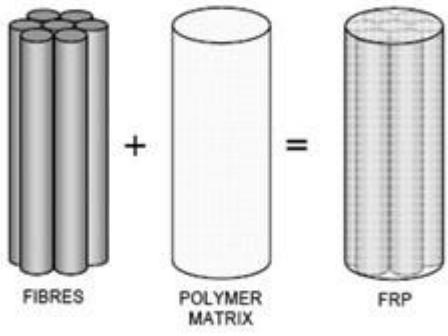

Figure 2.1: Component of an FRP bar (Said, 2014)

2.4 Manufacturing Process

“FRP bars are manufactured using a process called pultrusion” Kocaoz et. al, (2005). It involves making bundles of long parallel fibre of desired diameters which are then passed through container of liquid resin. They are then passed through a die and the fibres are then compressed and shaped into various bar sizes. The bars can then be subjected to different surface treatment such as making indentation, sand particle treatment or helical fibre wrapped around the bar to increase the bonding property of the final product. The pultruded process creates new properties that neither the fibres and the resins have on their own and at the same time preserving their individual chemical features (Jalil, 2014). FRPs exists in three forms;

1. As stirrups and longitudinal bars for internal reinforcement
2. As a structural elements on its own where it is entirely made of FRP
3. As wrapping sheet for strengthening beams and columns.

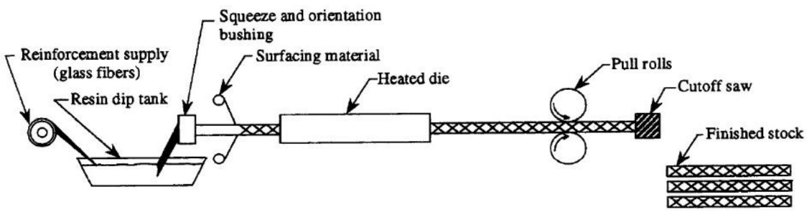

Figure 2.2: Pultrusion process (Benmoktane et al., 1995)

2.5 Types of Fibre Reinforced Polymer (FRP) Bar

The different types of FRP bars used in reinforcing concrete elements and they are based on the type of fibre used.

1. **Aramid fibre reinforced polymer (AFRP) bar**
   The fibre is derived from aromatic polyamide; a type of polymer.it was first introduced as Kevlar in the 1960s (Bhatnagar & Asija, 2016). Aramid fibres have low melting temperature, high moisture absorption, very low compressive strength and high initial cost. They are lighter than other FRPs and exhibits a very high energy absorption due to its higher strain of rupture and damping coefficient.
2. **Carbon fibre reinforced polymer (CFRP) bar**
   It doesn’t absorb moisture and have the ability to withstand more heat than AFRP. CFRP exhibits a very low thermal coefficient; an advantage for it to be used for

structures in in places open to extreme temperatures. They are more suitable for use in certain concrete structure due to their high tensile strength when compared with other FRPs.

3. **Basalt fibre reinforced polymer (BFRP) bar**

   This is a newly produced FRP, it is not as popular as the other types of bars. Basalt fibres have been used as sheet for external strengthening and bars for internal reinforcement. They have great performance towards chemical resistance and are harmless to the environment. It is inflammable and doesn't react with water.

4. **Glass fibre reinforced polymer (GFRP) bar**

   It is highly recommended in building due of its good insulating property, low cost and high resistance to certain chemicals. More detailed information will be discussed later in the thesis.

Figure 2.3: Samples of FRP bar (Maurizio, 2010)

2.6 Advantages and Disadvantages of FRP Bars

Fibre reinforced polymer (FRP) bars exhibits features which serves as a benefit or as a drawback. The advantage and disadvantages are stated below.

2.6.1 Advantages

The known advantage of FRP bars are as follows;

1. Higher tensile strength than mild steel
2. Lightweight (0.2 – 0.25 of the weight of steel bar)
3. Resistant to electrical and thermal conductivity (limited to GFRP bar only)

4. No need for admixtures that prevent corrosion
5. Endures high level fatigue
6. Longer service life in corrosive environment when compared to steel bar
7. Thickness of concrete cover can be reduced
8. Not affected by chemical attack and chloride ion
9. Better damage tolerance than steel bar coated with epoxy
10. More cost effective than steel bar coated with epoxy coated or galvanized steel bar

2.6.2 Disadvantages

The known disadvantages of FRP bars are stated as follows;

1. It doesn’t yield before rupture (exhibit brittle failure)
2. Low elastic modulus depending on the fibre type
3. Possibility of polymeric resin and fibres damage when exposed to ultraviolet radiation
4. Possibility of damage due to fire but depends on the type of matrix and thickness of concrete cover
5. Decrease in durability in alkaline environment for some aramid and glass fibres
6. Higher coefficient of thermal expansion
7. Lower creep - rupture limit when compared to steel
8. FRP is anisotropic while steel is isotropic

2.7 Fibre Reinforced Polymer (FRP) Properties

Fibre reinforced polymer (FRP) bars consist of materials each having its own properties which is combined to constitute a superior and modern reinforcing bar. The mechanical, physical and long-term behaviours the FRP bars are stated below.

2.7.1 Mechanical properties

A material’s property that requires a reaction due to an applied force. It helps in determining the range of usefulness of a material and establishes the expected service life. Identification and classification of a material is also aided by mechanical properties.

2.7.1.1 Compressive behavior

Designing of FRP reinforcement bars to resists compression stresses is not recommended (American Concrete Institute, 2015). The contribution of FRP to compressive stresses in negligible or non-existent and several experiments shows that the tensile strength is significantly higher than the compressive strength (Wu, 1990). This also applies to the elastic modulus; compressive elastic modulus is lower than the tensile elastic modulus. It is reported that the compressive elastic modulus is around 85% of CFRP, 80% of GFRP and 100% of AFRP of tensile elastic modulus of corresponding material (American Concrete Institute, 2015). The lower compressive modulus of elasticity comes from the fact that the compression test causes premature failure due to end brooming and micro-buckling of internal fibre.

According to ACI Committee 440, (2015), there is no standard test introduced to determine the behavior of FRP bars in compression.

2.7.1.2 Tensile behavior

Tensile strength is one of the important aspect of FRP bars. They doesn’t yield before rupture; they have linear behavior until failure without experiencing yielding. Figure 2.4 illustrates the stress strain relationship of the different types of fibre reinforce polymer bars and steel bar. Table 2.1 presents a summary of tensile properties of FRP bars.

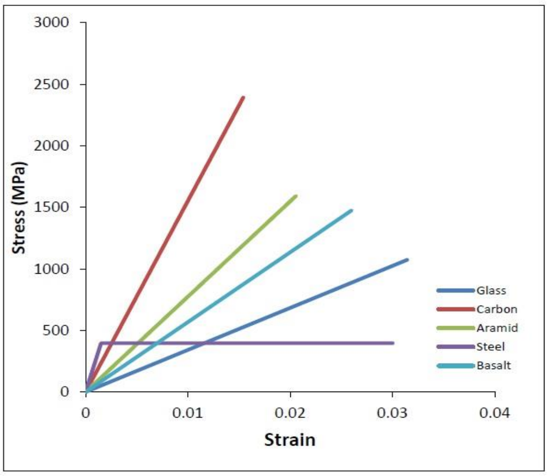

Figure 2.4: Stress strain curve of reinforcement bars (Fico, 2008)

Several factors are dependent on the stiffness and tensile strength of FRP bars. The strength of resin is lower than fibre, therefore the fibre-volume ratio to the total volume of an FRP bar and this is responsible for the tensile properties of the bar. Strength and stiffness of FRP bars vary with fiver-volume ratio. The element responsible for carrying load in an FRP bar is the fibre, therefore the ratio, orientation and the type of fibre used are the important aspects regarding tensile strength of the bar. Determination of curing rate, quality control and the manufacturing technique are also determined by the aforementioned characteristics of the fibre (American Concrete Institute, 2015).

The manufacturer should provide the tensile properties of the FRP bar. The manufacturer should also state clearly the guaranteed tensile strength(f_u). The GTS (f_u) is computed by subtracting thrice the standard deviation from mean strength $\left(f_u = f_{u,ave} - 3\sigma\right)$ and rupture strain$\left(\varepsilon^*_{u,ave}\right)$ is computed by$\left(\varepsilon^*_{u,ave} = \varepsilon_{u,ave} - 3\sigma\right)$. Also, guaranteed elastic modulus is stated as the mean modulus E_f $\left(E_f = E_{f,ave}\right)$ (American Concrete Institute, 2015).

Bending of an FRP bar is impossible after manufacture unless if a thermoplastic resin is used which makes it possible when heat and pressure is applied. The tensile strength of bars with bends experience a 40-50% strength reduction (Nanni & Gold, 1998).

It is known that FRP is of brittle nature and experience catastrophic failure without deforming, this avoids shrinking along the cross-section of the bar resulting in higher tensile strength (Salh, 2014).

Table 2.1: Tensile properties of steel and FRP bars (American Concrete Institute, 2015)

	STEEL	AFRP	BFRP	CFRP	GFRP
Nominal yield stress (MPa)	276 – 517	-	-	-	-
Tensile strength (MPa)	483 – 690	250 -2540	1200	600 – 3690	483 – 1600
Elastic modulus (GPa)	200	41 – 125	50	120 – 580	35 – 51
Yield strain %	0.14 – 0.25	-	-	-	-
Rupture strain %	6.0 – 12.0	1.9 – 4.4	2.5	0.5 – 1.7	1.2 – 3.1

2.7.1.3 Shear behavior

FRP bars are generally weak in shear. This is because layers of resin are not reinforced between fibre layers. The shear strength depends on the resin polymer which is weak and reinforcement across layers which is absent. The shear strength is also influenced by the orientation of FRP bars. Braided and twisted bars seems to have higher shear strength than straight bars due to varying orientation of the fibres present in the bars.

2.7.1.4 Bond behavior

This property depends on the manufacturing technique, design, environmental factors and the mechanical properties of the bar. Furthermore, the bond strength increase as the bar's diameter decreases and vice versa.

Bond force goes through the resin to reach the fibres and there is possibility of bond-shear failure in the resin. As tension increases in a deformed bonded bar, the adhesion existing between concrete and the bar is diminished. The surface of the bar deforms and this leads to inclined forces to acts between concrete and the bar. The stress existing on the surface of a bar is regarded as the bond stress acting between concrete and the FRP bar.

Many researchers determined the bonding properties extensively using various tests such as splice test and pull-out test to determine the embedment length equation (Benmokrane et.al, 1997).

2.7.2 Physical properties

These are the properties of the FRP bars that can be observed and measured, the physical properties are stated below.

2.7.2.1 Coefficient of thermal expansion

This property changes in the transverse and longitudinal paths, it depends on the resin, type of fibre and volume-ratio of fibre. The properties of the fibre is responsible for the longitudinal CTE. The longitudinal and transverse coefficient of thermal expansion of steel and FRP bars are stated in Table 2.2. It is important to keep in mind that materials that shrink as a result of increase in temperature and expands as a result of decrease in temperature have negative value of CTE. “The thermal expansion of FRPs in longitudinal direction is lower than in transverse direction, but the thermal expansion in transverse direction is higher than that of hardened concrete” (Masmoudi et. al, 2005).

“The strength of FRP fibre perpendicular to the fibre axis is ten times lower than the strength of a FRP fibre which is parallel to the longitudinal axis” (Salh, 2014).

Table 2.2: Coefficient of thermal expansion of steel bar and FRP bars (Salh, 2014)

	$CTE \times 10^{-6}/℃$				
Direction	**Steel**	**AFRP**	**BFRP**	**CFRP**	**GFRP**
Longitudinal, αL	11.7	-6.0 – -2.0	21/K	-9.0 – 0	6.0 – 10.0
Transverse, αL	11.7	60.0 – 80.0	-	74.0 – 104.0	21.0 – 23.0

2.7.2.2 Density

The density of FRP bars is low when compared to steel bars. This enables is to be easily transported and handled. It ranges from 1250-2150kg/m^3 which is 1/6 to ¼ to that of steel. Table 2.3 gives the densities of steel and FRP bars.

Table 2.3: Density of steel bar and FRP bars (Salh, 2014)

Types	Steel	AFRP	BFRP	CFRP	GFRP
Density (kg/m^3)	7900	1250 – 1400	1950	1500 – 1600	1200 – 2100

2.7.2.3 Effects of fire and high temperature

Consideration should be given to concrete flexural element reinforced with FRP bars as to how they respond to heat similar to how concrete elements reinforced with steel are considered (American Concrete Institute, 2015). According to ACI 440.1R-15 there is need for more research on the effects of higher temperature on the axial and shear capacity of FRP reinforced concrete elements.

Generally, use of FRP bars in areas prone to fire accidents is not advisable because at high temperatures the polymers becomes soft and cause a decrease in elastic modulus (Wang et. al, 2009). The components for FRP includes hydrogen, nitrogen and carbon atoms which are highly flammable and also releases harmful gases that are dangerous (Hollaway, 2010).

The concrete cover has an effect on the shear and flexural capacity of FRP RC elements when exposed to fire. There is also rapid decrease in flexural and shear resistance at elevated temperature. A minimum value of 64mm should be used for the thickness of concrete cover (Saafi, 2002).

2.7.2.4 Thermal conductivity

This property determines how at ease temperature passes through a material. For FRP bars, the thermal conductivity is generally low making them good insulators of heat. To increase the thermal conductivity of metallic filler are added to resin during polymerization (Hollaway, 2010).

2.7.3 Long-term behaviours

These are time dependent characteristics of the FRP bars which regards to strength, it is an important factor when designing reinforced concrete structures. These properties are stated below.

2.7.3.1 Creep rupture

Subjection of FRP bars to tension constantly through a significant time period will eventually experience catastrophic failure after exceeding the endurance limit, this occurrence is referred to as creep rupture or static fatigue. In steel bars used in reinforcing concrete, creep rupture effect is not an important aspect except in extreme temperatures.

In extreme environmental conditions like exposure to ultra violet radiation, drying and wetting cycles, elevated temperatures, freezing and thawing cycles or high alkalinity, FRP bar under static loading eventually fails over time (Salh, 2014).

Glass fibres performs poorly in creep rupture, then aramid fibres. Carbon fibres performs better in creep rupture when compared to other fibres and it all depends on environmental factors like moisture and temperature (American Concrete Institute, 2015).

2.7.3.2 Fatigue

There are various amount of data for the past 30 years stored on the lifespan and fatigue of FRP but limited to aviation industries. No enough researches related to RC elements (American Concrete Institute, 2015). Reports explained that among all type of FRPs, GFRP is less prone to fatigue. At about a million cycle, there is a 30-50% decrease in fatigue strength when compared to initial static strength. AFRP bar in concrete tends to lose 27-46% of its tensile strength at about 2 million cycles (American Concrete Institute, 2015).

Fatigue behavior is strongly dependent on environmental conditions such as alkalinity, acidity and moisture in the concrete mass covering the bars. Fatigue limit cannot be clearly determined unlike steel (Rahmatian, 2014). It is important to keep in mind that degradation of resin or fibre interface under alkaline and moist environment can have a detrimental effect. Generally, behavior of fatigue in FRP largely depend on the bond between resin matrix and fibre.

2.7.3.3 Durability

Durability of FRP reinforced concrete element is dependent upon many factors such as water, acidic or alkaline solutions, elevated temperature, saline solutions and ultraviolet exposure. Stiffness and strength varies or remain constant which depend on the exposure condition or type of material. Bond and tensile properties are the most important parameters of FRP bars that needs to be regarded during construction of reinforced concrete structures (American Concrete Institute, 2015).

2.8 Glass Fibre Reinforced Polymer (GFRP) Bar

A type of FRP bar that is comprised of large amount continuous tiny fibres of glass held together in a matrix of polymeric resin. GFRP has been recommended to be used in numerous structural application due to its non-corrosive nature when compared to steel bar. Other interesting benefits includes chemical attack resistance, high stiffness and strength to weight ratio, good fatigue properties, control over damping characteristics and thermal expansion and resistant to electromagnetic waves (Abdalla, 2002). Other types include AFRP, BFRP and CFRP.

Other than the good physical and mechanical properties, FRP bars are also regarded as cost effective when compared to steel bar especially when corrosion is of concern (Worner, 2015).

S-glass (high strength and modulus) and E-glass (electric/conventional type) are the most common type of fibre used in making GFRP bar and the resins to be used depends on the rigidity, strength, cost and long term stability (Worner, 2015). The fibres are responsible for the strength and stiffness of the bar while the polymeric resin hold the fibre in place to enable transfer of stress between them. To gain the highest possible tensile strength, orientation of the fibre should be the same as the longitudinal direction of the bar although different orientation of fibres are adopted by other manufacturers (Worner, 2015). Other types of glass fibre include C-glass (chemically resistant) and A-glass (alkali resistant) (Jalil, 2014). To increase the bonding strength, different types of bars where introduced as shown in Figure 2.5 which are smooth bar, ribbed bar, helical fibre wrapped bar and sand coated bar (Worner, 2015).

Table 2.4 shows the types of glass fibre with their given full name and Table 2.4 presents the chemical components of the various types of GFRP.

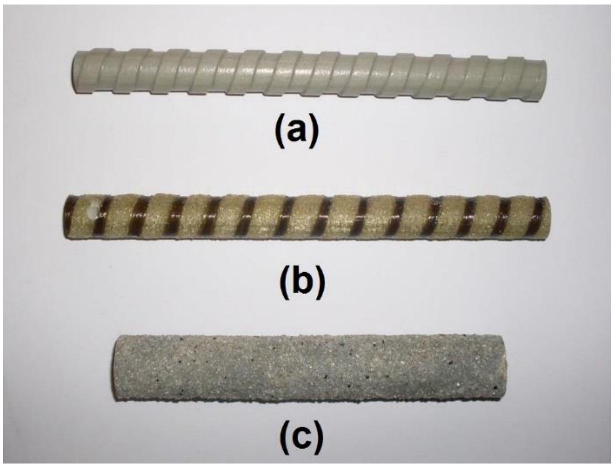

Figure 2.5: Types of bar surface (Fico, 2008)

Table 2.4: Types of glass fibre (Fico, 2008)

Type	Full Name
E-Glass	Standard conventional glass type
S-Glass	High strength and high modulus glass
C-Glass	Chemical resistant glass
ECR Glass	Chemically resistant conventional glass
A-Glass	Alkali resistant glass

Table 2.5: Chemical composition of different types of GFRP (ACI 440.1R-15, 2015)

% of components	A-Glass	C-Glass	E-Glass	ECR-Glass	S-Glass
SiO_2	54	60	60 – 65	54 – 62	62
CaO	20 – 24	14	14	21	5 – 9
Al_2O_3	14 – 15	25	2 – 6	12 – 13	-
MgO	-	3	1 – 3	4.5	1 – 4
B_2O_3	6 – 9	< 1	2 – 7	< 0.1	< 0.5
K_2O	< 1	< 1	8	0.6	-
Na_2O	-	-	-	-	12 – 15
ZrO_2	-	-	-	-	17

As seen in the table, the predominant element present in all the types of glass fibre is silicon. Silicon provides the fibre with strength but it also has a drawback as they are involved in chemical reaction where hydroxyl ions are present. This reaction degrades the fibre matrix resulting in degradation of inner structure of the rebars.

Kocaoz et. al, (2005) tested GFRP bars having 4 different types of coating and tensile behavior and found out that coating of a bar has an effect on its tensile strength.

It is known that increase in diameter of GFRP leads to decreasing tensile strength as a result of shear lag effect, therefore bars of different diameters have different tensile strength. The bar size does not have an effect on the elastic modulus, but it is affected by the volume of fibre present (Kocaoz et al., 2005).

The GFRP bar to be used in this study has a guaranteed tensile strength of 1250 MPa. The initial steep slope of the steel bar curve is as a result of the high elastic modulus of steel. But it also showed that GFRP bar is able to withstand more stress than steel bar (Worner, 2015).

2.9 GFRP Applications in Civil Engineering

There is a wide range of application of GFRP composite in the Engineering aspects but below are applications regarding the Civil Engineering field.

2.9.1 Parking garages

Generally, parking garages are exposed to corrosion because vehicle carries salt and water from the environment on their body. GFRP is an ideal material for constructing parking garages (TUF-BAR, 2018).

A parking garage in Quebec, Canada named La Chanceliere was deteriorating due to corrosion. It consists of two way slab system where the internal steel bar is heavily corroded (Figure 2.6a). Proposal was made for rehabilitation to use GFRP bar as reinforcement in the slabs but the columns and the walls were maintained. Initially, two designs were prepared; with steel bars and GFRP bars. Initial cost of GFRP design was higher than the steel design but the GFRP design was still adopted because cost analysis showed that cost effectiveness can be achieved with the GFRP design (Ahmed et. al, 2016).

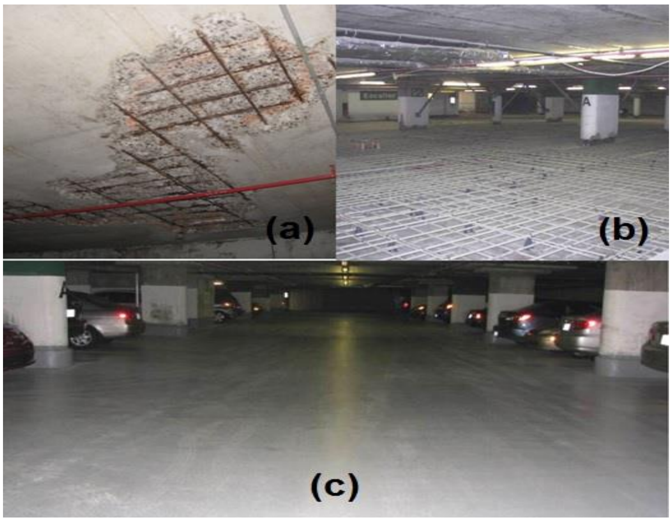

Figure 2.6: La Chanceliere Parking Garage in Quebec, Canada (a) Corroded steel in Slab, (b) Placement of GFRP reinforcement, (c) Parking Garage in Service (Ahmed et al., 2016)

2.9.2 Bridges

Repair and maintenance of bridges is very expensive. When steel bars are exposed to deicing chlorides, the service of the structure is reduced. Bridges are open to environmental and stress factors. GFRP bars are designed in such a way there are able to sustain heavy traffic loads and also natural disasters like earthquakes. GFRP bars used in constructing bridges certainly reduces cost of maintenance (TUF-BAR, 2018)

The first bridge for transportation in the United States constructed using GFRP bar was in 1996 in Mckinleyville Brooke County. It was recommended because of its benefit in terms of its serviceability under fatigue and static loads when used as internal reinforcement in concretes (Thippeswamy, Franco, & GangaRao, 1998).

Figure 2.7: Bridge Deck in Morristown – Vermont, USA (Fico, 2008)

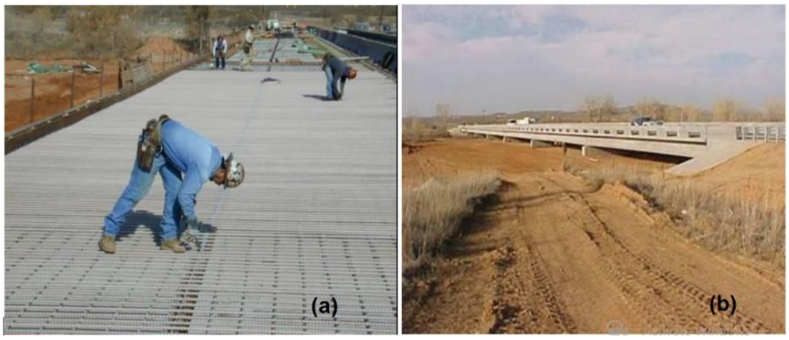

Figure 2.8: Sierrita de la Cruz Creek Bridge, Potter County, Texas (a) Under construction (b) In service (Salh, 2014)

Figure 2.9: GFRP Bridge Deck, Cookshire-Eaton, Quebec (a) Under construction (b) In service

2.9.3 Rail

As population grows, there is need for increase in the capacities of public transportation. Generally, magnetic or conductive materials should not be used at all or in small quantity around electric trains, this makes GFRP bars an ideal material to be used in railways. GFRP bars has been proven to be an excellent material for rail systems.

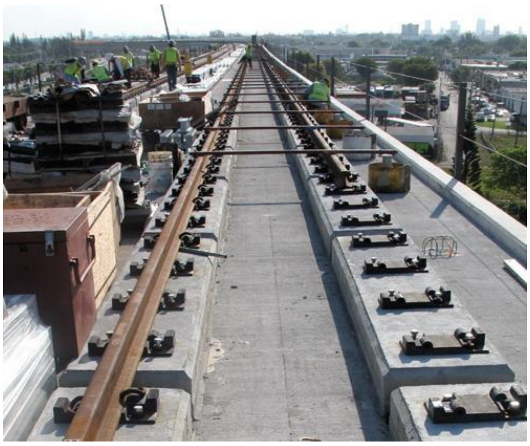

Figure 2.10: GFRP as railway plinths (Composites World, 2011)

2.9.4 Airport runways

With years airplanes are getting heavier and bigger. Achieving longer service life should be regarded when it comes to airport runways. GFRP bars used in reinforcing runways helps in withstanding the landing impact of airplanes which can be over 500,000 pounds. Flexibility and strength standards should be strictly adhered to when constructing concrete base of airport runways. Reinforcing runways using GFRP bars makes it to be durable, flexible and strong. It is not advisable to use traditional steel for runways. GFRP bars can main the runway's integrity for over 100 years (TUF-BAR, 2018).

2.9.5 Medical and information technology

Medical and IT facilities contain equipments that emits magnetic waves or require massive electric currents, this calls for non-magnetic, non-metallic and non-conductive materials to be used in constructing these facilities to avoid interference with delicate circuit or machines. Also, the GFRP bar has twice the tensile strength of the steel bars (TUF-BAR, 2018).

Figure 2.11: MRI room in Lincoln General Hospital, NE, USA (Aslan FRP, 2018)

Figure 2.12: Trauma Centre in York Hospital, USA (Aslan FRP, 2018)

2.9.6 Seawalls

Seawalls are vertical structures erected to protect the environment against upland erosion and flooding. Seawalls and other marine structures like floating marine docks, water breaks, artificial reefs and buildings near the sea are generally reinforced using steel bars which make them sensitive to salts and chlorides thereby damaging the structures. GFRP bar is corrosion free and exhibits higher strength making it an ideal materials for marine application (TUF-BAR, 2018).

Figure 2.13: Seawall restoration in Palm Beach Florida, USA (Aslan FRP, 2018)

Figure 2.14: Seawall of Lyles residence in California, USA (Aslan FRP, 2018)

2.9.7 Unique structures

There are some special structures around the world which serve as a landmarks mainly because of their unique character and appearance. Some of the unique structures made using glass fibre reinforced polymer (GFRP) bar can be seen in Figures below.

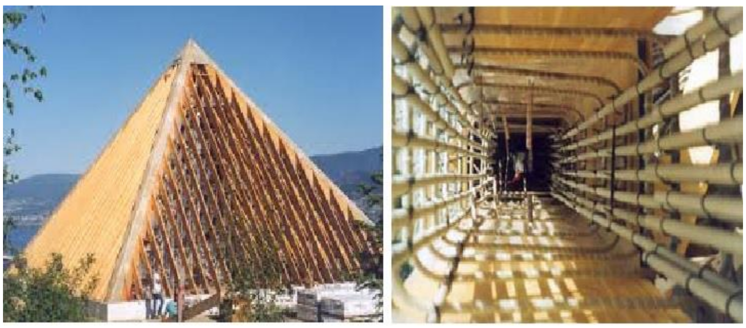

Figure 2.15: Pyramid shaped winery in British Columbia (Aslan FRP, 2018)

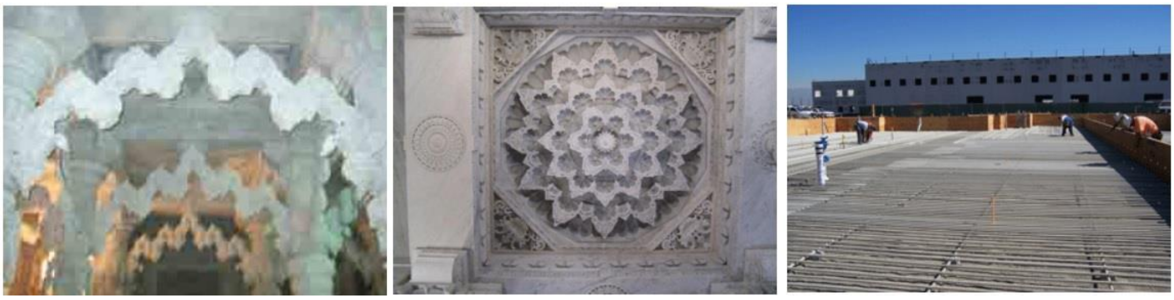

Figure 2.16: Hindu temple design with service life of 1000 years (Aslan FRP, 2018)

2.9.8 Precast

Same way RC elements are susceptible to corrosion so is precast concrete. Using GFRP as reinforcement in precast concrete increase the service life to over 100 years. GFRP bars are non-metallic thereby making precast concrete elements to be non-corrodible and to avoid discoloration by rust stain. It also makes it lighter (TUF-BAR, 2018).

Figure 2.17: Culvert bridge in City of Rolla, Phelps County, Missouri (Nanni, 2000)

2.10 Previous Experimental Studies

Shanour et al., (2014) performs experiment on beams having dimensions of 120x300x2800mm reinforced using locally made GFRP bars and steel reinforced beams. The main parameters of concern they regard was the impacts of compressive strength, the ratio of reinforcement and the type of material used (Steel or GFRP). The beams were subjected to four point bend tests and concluded that mid span deflection and crack width was reduced by increasing the ratio of reinforcement. Also, the ultimate capacity of the beam significantly increased as the reinforcement ration increases.

Ashour (2006) experiments on 12 GFRP reinforced beams having a span length of 2100mm under a four point loading system. Flexural and shear failure were observed, the flexural failure was due to tensile rupture of the GFRP bar while the shear failure is experienced in the shear span of the beam due to a large diagonal crack.

Brown (2006) performed an experimental work to determine how glass fibre reinforced polymer (GFRP) bars behave when used in reinforced concrete compression members. The beam specimens were subjected to compressive load until failure and results were compared which shows GFRP to be technically feasible; columns reinforced with GFRP yields about same capacity when compared to columns reinforced with steel of equal areas and using GFRP stirrups improves the bending capacity of the longitudinal bars.

Balendran et al., (2004) tested 18 beams with sand coated GFRP and mild steel as reinforcement in flexure and results were compared, the ultimate tensile strength of GFRP was found to be 2.5 times the steel and elastic modulus of GFRP was one fourth (25%) that of steel. But the GFRP reinforced beams experience larger deflections than steel reinforced beams. The generally low modulus of elasticity has been viewed as an important engineering disadvantage as GFRP reinforced concrete members may experience a bigger deflection than steel reinforced concrete members but based on tests by Masmoudi et al. (1995), the deflection is found to be 3 times that of steel at same level of load.

Micelli & Nanni, (2004) proposed an experimental protocol to examine the outcome of accelerated ageing on fibre reinforced polymer bars. Resin properties greatly affect the durability of the FRP bars, and when there is no enough protection by the resin to the fibres GFRP bars are exposed to alkaline attack.

Chidananda & Khadiranaikar, (2017) performs experiments on 12 beams having dimensions of 150x180x1200mm which is subjected to four point test. The beams where in 4 groups each with different ratio of reinforcement. They also concluded that increasing the ratio of reinforcement elevates the ultimate capacity of the beams and also shows how applicable the ACI standard is in beam design.

Saikia et al., (2005) carried out an experimental work to check the behavior of hybrid (GFRP and steel) bars used as reinforcement longitudinally on beams made with normal strength concrete.

Most experiment done either experiment or analytical shows GFRP to be better alternative in terms of flexural behavior but according to George & Parappattu (2017) the results of experimental work to compare GFRP and steel in reinforced beams shows steel to be better material in terms of flexural behavior when the area of reinforcement required for steel is 1.94 times GFRP reinforced beam having same moment capacity.

Kheni et. al, (2016) performs an experimental and analytical study to study the how GFRP RC element behave in comparison to steel RC element. Concrete beams where made with 20MPa and 25MPa concrete and also different reinforcement size combination. The analytical study was performed using finite element modelling software (ATENA 3D) to simulate each of the beams. Comparing the two results shows the ultimate capacity of GFRP reinforced beam is higher than steel reinforced beam. They also suggested that combining steel and GFRP bars together will result to much higher ultimate capacity.

Shin et. al, (2009) carried out a four point bend test on beams reinforced with steel bars and GFRP bars, they focused on reinforcement ratios and the strength of concrete. The displacement, crack width and strain of the 2 types of beams were recorded, GFRP reinforced beams experienced larger strains and displacements. They found out that concrete strength has an insignificant effect on crack width and crack spacing. They concluded that GFRP over reinforced beams are safer for designing especially when deformability is taken into account.

Barris et. al, (2012) experimented on GFRP reinforced concrete beams to determine their short term behavior in flexure using distinct ratio of reinforcement and varying the effective depth to height ratio. They examined some prediction models and try to compare them with experimental results. They concluded that the beam behaved linearly until cracking as a result of absence of plasticity of GFRP bar, but the failure is experienced at larger displacements. The prediction by ACI 440.1R regarding flexural load at service load level closely agree to the experimental result but that is not the case in higher load levels. The crack width from experimental result closely fits the minimum value proposed by ACI 440.1R which signified good bonding between GFRP bars and concrete. All beam failed as a result of concrete crushing and the experimental ultimate capacity of the beam was more than expected as per the ACI standard.

CHAPTER 3

FAILURE IN SIMPLE BEAM AND GFRP DESIGN GUIDELINES

3.1 Introduction

This chapter explains the modes of failure that is experienced in a simple beam and conditions that governs the occurrence. The chapter will also explain the design guidelines as per ACI 440.1R-15.

3.2 Flexural Failure

This is a type of failure that occurs as tension cracks propagates and as principal stress within the beam approaches the tensile strength of the concrete. If a beam is adequately reinforced but subjected to load that surpass the ultimate capacity of the beam, yielding of the reinforcement bar occurs which results to failure of the concrete, this is referred to as flexural failure. Reinforcement bar yields as a result of excessive stresses in the beam which is higher than the yield point of the reinforcement bar, this makes the tension cracks to upwardly propagate and becomes visible as the beam deflects. As the ultimate bending capacity is exceeded, flexural failure occurs and it is experienced in the region where the moment is at maximum. Flexural failure is preferred than other mode of failures as it happens gradually and is followed by the visible cracks which increases as the beam deflects more. Figure 3.1 illustrates the flexural failure which shows how the vertical cracks are experienced mid-span of the beam which results in stress redistribution (Nilson et. al, 2010).

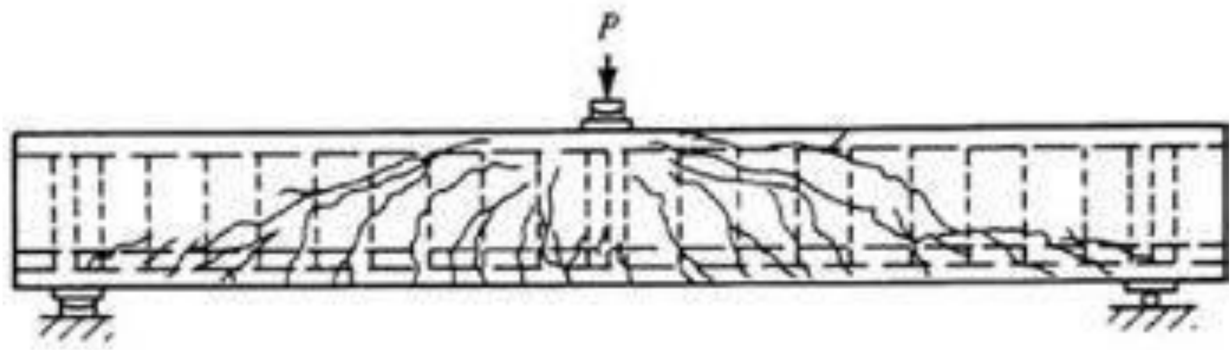

Figure 3.1: Illustration of flexural failure (Said, 2014)

3.3 Diagonal Tension Failure

It is also referred to as shear failure. Its occurrence is catastrophic and hazardous. It occurs unpredicted and progress rapidly, that is why it is the most undesired mode of failure. Shear failure is one of the major issue regarding concrete beams. Through the year, its causes and how it occurs has to be studied through experimental tests to understand the phenomenon better. The failure mechanism depend on certain parameters such as geometry, dimension, properties of the member and loading types. Diagonal crack are the main causes of the diagonal tension failure, it is experienced around the supports area and as a result of larger shear forces. As shown in Figure 3.2, the diagonal crack initiates when midspan flexural cracks ends and it happens at the direction of the concrete at support and reinforcement bar. As the cracks propagate to the region of high shear force which is close to the support, the beam suddenly fails (Nilson et al., 2010).

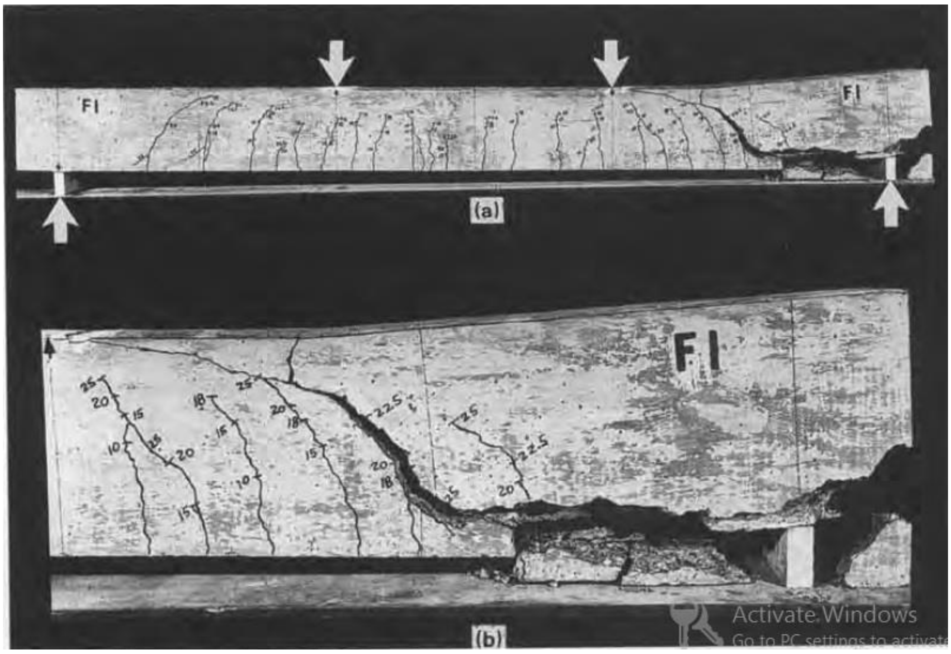

Figure 3.2: Diagonal tension failure of concrete beam (a) whole beam view (b) near support view

3.4 Shear Compression Failure

This type of concrete failure is experienced as diagonal crack due to shear forces propagates and reach the compression area with no warning in the form of secondary cracks as it is experienced in diagonal tension failure. It also cause concrete crushing to above the tip of the inclined crack close to the compression flange as illustrated in Figure 3.3. This failure is usually attributed to short beams (Nilson et al., 2010).

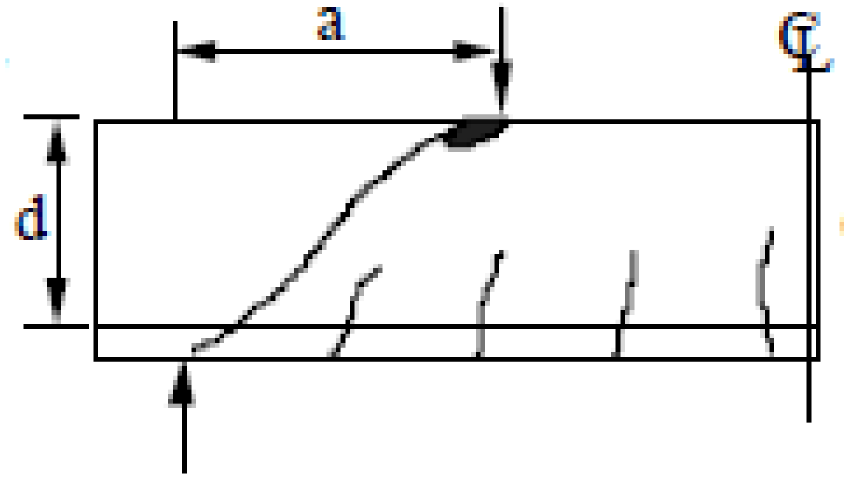

Figure 3.3: Illustration of shear compression failure (Said, 2014)

3.4 Design Philosophy

Design guidelines for FRP reinforced concrete beams is the same as the design guidelines for steel reinforced concrete beams but incorporating the variations in mechanical behavior of the FRP reinforcement bars. FRP bars does not go through plastic deformation which therefore requires some modifications in concrete beam design unlike steel bars that exhibits plastic behavior. Several guidelines have been developed over the years in Europe, Canada (CSA-S806, 2002; ISIS, 2001), Japan (JSCE, 1997) and USA (ACI 440.1R, 2001, 2003, 2006, 2015) (Salh, 2014).

3.4.1 Flexure limit state

The design guidelines of ACI for steel reinforced concrete elements (ACI 318-11) was modified to produce the design guidelines for FRP reinforced concrete elements (ACI 440.1R-15). The FRP bar design guidelines is based upon the fact that FRP behaves in a brittle manner. With regard to FRP reinforced concrete member, concrete crushing or FRP rupture is accepted as long as the required serviceability and strength is achieved. Due to absence of ductile behavior in FRP reinforced concrete members, it is suggested that safety factor higher than that of steel reinforced concrete element should be used (Nanni, 2000).

FRP is generally known to be a material of brittle elastic nature, it behaves linearly until failure with no yielding stage. This makes failure by concrete crushing to be more accepted than FRP rupture failure. This is the reason why the steel resistance factor 0.9 that also account for under reinforced members can't be adopted in concrete members reinforced with FRP bars. FRP reinforced concrete members make use of two resistance factor; 0.55 for under reinforced concrete members and 0.65 for over reinforced concrete members.

Environment factors (C_E) depending on the exposure condition where introduced for different types of fibres which are multiplied by the guaranteed strength and guaranteed strain at failure to get the design strength (f_{fu}) and design strain at failure (ε_{fu}). Table 3.1 presents the environmental factors associated to each fibre type at different exposure condition.

Table 3.1: Environmental factor of reduction under different condition of exposure

Exposure condition	Type of Fibre	Environmental factor of reduction C_E
Concrete not exposed to weather and earth	Aramid	0.9
	Carbon	1.0
	Glass	0.8
Concrete exposed to weather and earth	Aramid	0.8
	Carbon	0.9
	Glass	0.7

The capacity of a FRP member flexure depends on either concrete crushing controlled of FRP rupture controlled. Calculating the ratio of reinforcement and balanced reinforcement ratio determines which of the conditions controls. The FRP reinforcement ratio is calculated by;

$$\rho_f = \frac{A_f}{bd} \tag{1}$$

The balanced reinforcement ratio is calculated by;

$$\rho_{fb} = 0.85\beta_1 \times \frac{f'_c}{f_{fu}} \times \frac{E_f \varepsilon_{cu}}{E_f \varepsilon_{cu} + f_{fu}} \tag{2}$$

The design tensile strength is used to calculate the balanced reinforcement ratio because FRP does not undergo yielding. If the FRP reinforcement ratio is greater than the balanced reinforcement ratio, it is controlled by concrete crushing while if it is less than the balanced reinforcement ratio, FRP rupture controls. The distribution of stress in concrete can be determined using the rectangular stress block of ACI and depending on the strain compatibility and equilibrium of forces, the flexural strength equation is derived.

The nominal flexural strength of concrete is calculated when concrete crushing controls, using the tensile stress of the FRP bar (f_f). It is given as;

$$f_f = \sqrt{\frac{(E_f \varepsilon_{cu})^2}{4} + \frac{0.85\beta_1 f'_c}{\rho_f} E_f \varepsilon_{cu}} - 0.5 E_f \varepsilon_{cu} \tag{3}$$

$$M_n = A_f f_f \left(d - \frac{a}{2}\right) \tag{4}$$

$$a = \frac{A_f f_f}{0.85 f'_c b} \tag{5}$$

When concrete is controlled by rupture of FRP reinforcement, the nominal flexural strength is calculated using design tensile stress of the FRP bar (f_{fu}). It is given as;

$$M_n = A_f f_{fu}\left(d - \frac{\beta_1 c}{2}\right) \qquad (6)$$

In doubly reinforced concrete containing FRP bar in the compression zone, the effect of the FRP bar regarding flexural strength is negligible and therefore should be neglected. Generally, an under reinforced member will fail by FRP rupture while an over reinforced member fails by concrete crushing.

As calculations can be used to predict the crushing limit state of concrete but the failure of the member might be different. For instance, FRP rupture might control a section if the strength of concrete is greater than the specified strength. This makes it important to introduce a transition in between the values of φ. An FRP RC section that is compression controlled is a section that satisfies $\rho_f \geq 1.4\rho_{fb}$ and FRP RC section that is tension controlled is a section that satisfies $\rho_f \leq \rho_{fb}$. Theoretically, crushing limit state controls a section that satisfies $\rho_{fb} < \rho_f < 1.4\rho_{fb}$, this results to a lesser value of φ which is relative to a section that is compression controlled.

Flexural strength reduction factor is calculated using equation (7) and it is shown graphically in Figure 3.4. A factor of 0.55 is used for sections that are tension controlled while a factor of 0.65 is used for sections that are compression controlled, a formula to calculate the transition between the two conditions is also provided.

$$\begin{cases} 0.55 \quad for\ \rho_f \leq \rho_{fb} \\ 0.3 + 0.25\frac{\rho_f}{\rho_{fb}}\ for\ \rho_{fb} < \rho_f < 1.4\rho_{fb} \\ 0.65 \quad for\ \rho_f \geq 1.4\rho_{fb} \end{cases} \qquad (7)$$

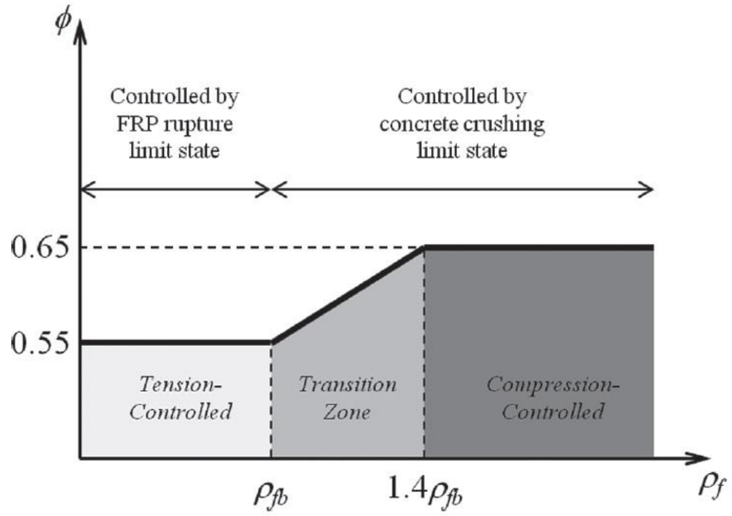

Figure 3.4: Reduction factor of strength (American Concrete Institute, 2015)

Concrete section having small amount of reinforcement than the balanced reinforcement ratio fails by FRP rupture and the section is tension controlled, therefore the minimum amount of reinforcement required should be determined to avoid failure upon cracking of the concrete. The formula provided by the ACI 318 code is similar to the formula for FRP reinforced members but with some modifications, which is due to different factors of strength reduction; 0.9 for the steel reinforced members while 0.55 for the FRP reinforced members. It is given as;

$$A_{f\,min} = \frac{0.41}{f_{fu}}\sqrt{f_c'}\,b_w d \;\; \geq \;\; \frac{2.3}{f_{fu}}\,b_w d \qquad (8)$$

If a concrete section is compression controlled$(\rho_f > \rho_{fb})$, the minimum reinforcement amount needed to avoid failure upon cracking is achieved automatically and so checking the minimum reinforcement is not required.

3.4.2 Serviceability limit state

FRP reinforced beam experience bigger deflections than steel reinforced beams having the same geometry and reinforcement ratio. This results to larger cracks along the span of the beam thereby decreasing the stiffness and results in extensive deflection.

3.4.2.1 Cracking

Crack width becomes unaesthetic when it is excessive and also results to problems that leads to degradation or damage of concrete.

Modifications were made to provisions for serviceability in ACI 318 for crack control to consider the increase of flexibility when using reinforcement exhibiting low stiffness. FRP bars are resistant to corrosion unlike steel bars, this makes the extensive cracks attributed to FRP reinforced beams to be tolerated when compared to steel reinforced beams when the basis for crack control is corrosion. Crack width consideration is important when creep rupture, shear effects and aesthetics are regarded.

The methodology used to control flexural crack involves computing the crack width using equation provided by ACI 440.1R and the value is compared with the maximum allowable crack width. The following equation can be used to compute the maximum allowable crack width according to ACI 440.1R;

$$w = 2\frac{f_f}{E_f}\beta k_b\sqrt{{d_c}^2 + \left({}^{s}/_{2}\right)^2} \qquad (9)$$

The Japan Society of Civil Engineers, (1996) focus their basis on aesthetics and proposes 0.5mm as the maximum allowable crack width. CAN/CSA-S6-06 proposes a value of 0.7mm for beams in normal environments and 0.5mm for beams in aggressive environments. According to ACI 440.1R, if crack width are based on aesthetic conditions, an acceptable range from 0.4 to 0.7mm is adopted.

CHAPTER 4

EXPERIMENTAL STUDY

4.1 General

This chapter gives the detailed description of experimental works that are carried out in this thesis, they were done in the KKTC Chambers of Civil Engineers laboratory. The details of test specimens which includes the geometry, reinforcement details and how the specimens are prepared is clearly stated. The specimens will be subjected to compression test, pull-out test and flexural test and the procedure are clearly stated. Material properties of GFRP bar and steel bar are also tested and stated.

4.2 Materials

4.2.1 Concrete

A C30 grade concrete was used for the whole experimental works. It was obtained from the construction site of the new Near East University mosque supplied by Kofali Beton Company.

4.2.2 Steel bars

The steel reinforcing bars of diameters 8mm, 10mm and 12mm were used for the various part of the experimental works.

4.2.3 Glass fibre reinforced polymer (GFRP) bars

The GFRP reinforcing bar used for this experimental works is part of the Liana composite products produced by Ural Reinforcing Company which is based in Russia. GFRP bars of diameters 8mm, 10mm and 12mm were used for the various parts other of the experimental study. The ultimate tensile strength of the GFRP bar as provided by the manufacturer is 1250Mpa.

4.3 Equipment

4.3.1 Automatic compression machine

An automatic compression testing machine manufactured by UTEST with model number UTC-4320 was used for the concrete compression test. It has a load capacity of 200kN and BC 100 control units.

Figure 4.1: Compression testing machine (UTC-4320)

4.3.2 Universal testing machine

A universal testing machine manufactured by UTEST with model number UTM-4000 was used for the tensile test to determine the material properties of the reinforcing bars. It has a load capacity of 600kN and BC 100 control units.

Figure 4.2: Universal testing machine (UTM-4000)

4.3.3 Pull-out test apparatus

The apparatus is made with 10mm thick steel and in such a way it can fit into a universal testing machine. It is shown in Figure 4.3

Figure 4.3: Pull-out apparatus

4.3.4 Flexural testing machine

An automatic flexural testing machine manufactured by UTEST with model number UTC-4620 was used for the four point bend test. It has a load capacity of 200kN.

Figure 4.4: Automatic flexural testing machine (UTC-4620)

4.4 Test Procedures

This section present an extensive details of the test procedures used for the experimental works. The test procedures includes the tensile test of reinforcing bars, preparation of reinforcement cages, the casting of concrete cubes for pull-out test and compression test, the casting of the beams for four point bending test.

4.4.1 Testing reinforcing bars

The tensile testing of steel bars was performed according to British Standard (BS EN ISO 6892-1) and GFRP bars according to ASTM standard (D7205/D7205M-06) to determine the ultimate stress, percentage elongation and modulus of elasticity. A constant pace rate of 0.6MPa was used for application of load on the steel bars, while displacement type load rate of 1mm/min was used on the GFRP bars, both reinforcement bars where loaded until failure.

In preparing GFRP bars anchors are need in order to prevent damage due to the grips of the tensile testing machine, steel tubes are used and filled with either cement grout or epoxy whom have good compressive strength. The schematic diagram of the specimen is shown in figure 4.6.

Figure 4.5: GFRP bar specimen

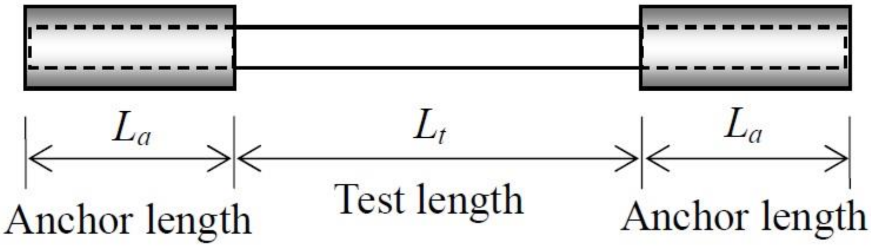

Figure 4.6: Schematic diagram of GFRP bar specimen

4.4.2 Testing concrete cube strength

The concrete compression test was performed according to British Standards (BS EN 12390-3). C30 grade of concrete was used for the casting the concrete cubes. The concrete was poured vertically into the mould of dimensions 15x15x15mm and compacted using a rod. The hand compaction was done gently to remove entrained air during concrete pouring. The concrete cube was removed from the mould after 24 hours and inserted in a curing tank containing water under 20±2°C and 100% relative humidity. After 28 days, the cubes were removed from the curing tank and inserted in the automatic compression test machine for testing. A constant pace rate of 0.6MPa/s was used for loading and the cube was continuously loaded until failure.

Figure 4.7: Concrete cube moulds and casted specimens

The compressive strength of concrete cube was determine using the equation;

$$f_c' = \frac{F}{A_c} \tag{10}$$

Where f_c' is the compressive strength, F is the maximum load at failure and A_c is the cross-sectional area. The overall results obtained from the concrete cube strength test is stated in Table 4.1

Table 4.2: Concrete strength of cubes

Specimen	**Mass (kg)**	**Compressive strength (MPa)**
C1	12810	37.21
C2	12730	32.55
C3	12790	33.44
Average	12776.7	34.4

4.4.3 Testing bonding behaviour

Pull-out test was performed using an apparatus in a universal testing machine. The test was performed according to American Standard (ASTM C234-91). The specimen was prepared similar to the concrete cube. Φ10 GFRP and steel bars of 300mm long was inserted at the centre of cubes after concrete pouring at a depth of 100mm. After 28 days curing, the specimens were inserted in the pull-out apparatus and placed in the universal testing machine. The load was applied at a constant pace rate of 1mm/min until failure. The ultimate bond strength was computed using equation below;

$$\tau_b = \frac{P_{max}}{\pi D L} \quad \text{(MPa)} \tag{11}$$

Where τ_b is the ultimate bond strength, P_{max} is the ultimate pullout load, D and L is the diameter and embedded length of reinforcing bars. Schematic description of the pull-out specimen is shown in Figure 4.7a.

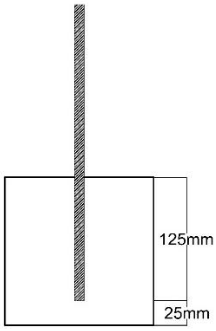

(a) Details and dimensions of pull-out specimen

(b) Casted pull-out specimens

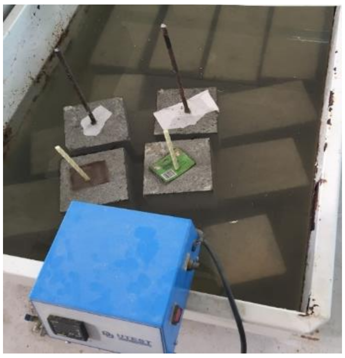

(c) Curing of pull-out specimens

Figure 4.8: Preparation of pull-out specimens

4.4.4 Testing flexural behaviour

The overall procedure carried out in preparing the beam specimens for flexural testing is presented below.

4.4.4.1 Description of beam specimens

A beam with 300x300mm sectional dimensions was adopted at the beginning. But the beams used were prepared by adopting the scale of 1:2 making the sectional dimension to be 150x150mm. The beams were prepared in two groups; group 1 beams were reinforced with steel bars and group 2 beams were reinforced with GFRP bars. The summary of the beam details is shown in Table 4.1

Table 4.3: Beam details

Group	Specimen name	Type of reinforcement	Reinforcement ratio	Number of reinforcement		Stirrups (steel)
				Bottom	Top	
1	G1-BM1	Steel	1	2φ10	1φ8	φ8 @ 100
	G1-BM2	Steel	1.4	2φ12	1φ8	φ8 @ 100
	G1-BM3	Steel	2.1	3φ12	1φ8	φ8 @ 100
2	G2-BM1	GFRP	1	2φ10	1φ8	φ8 @ 100
	G2-BM2	GFRP	1.4	2φ12	1φ8	φ8 @ 100
	G2-BM3	GFRP	2.1	3φ12	1φ8	φ8 @ 100

4.4.4.2 Geometry of the beam specimens

The design of beams were done according to American Concrete Institute Code (ACI 318-11). The beams have dimensions 750x150x150mm, concrete cover of 25mm was used for all the reinforced concrete beams. The beams were in 2 groups; group 1 reinforced with steel bars while group 2 reinforced with GFRP bars. The beams were all designed in a way to be strong in shear. The geometry of beams each used for the GFRP and steel beams is shown in Figures 4.9. Parameters that were used in the beam design calculations are shown in Table 4.2. The detailed beam design calculations are shown in Appendix 1.

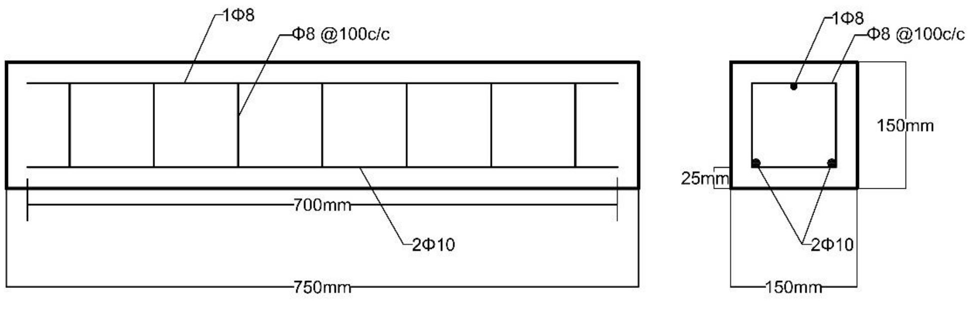

(a) Beam 1

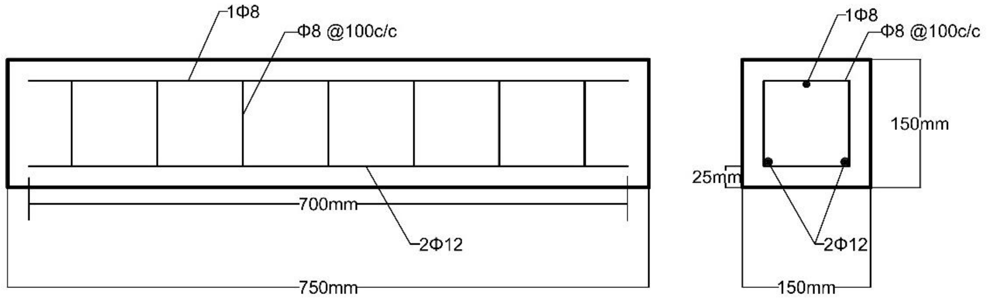

(b) Beam 2

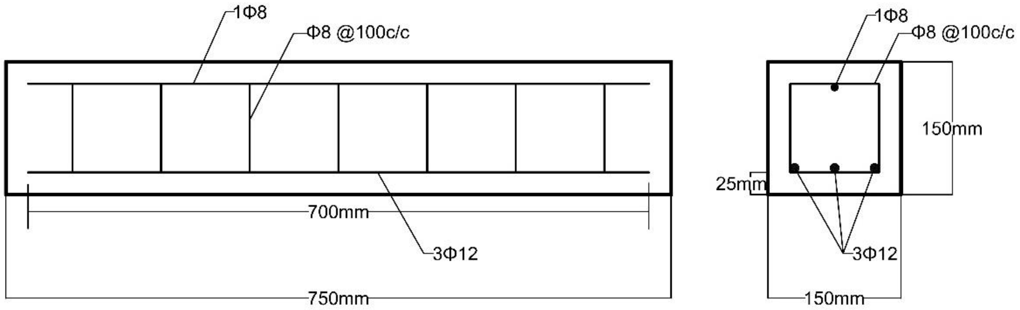

(c) Beam 3

Figure 4.9: Details and dimensions of all group 1&2 beams

Table 4.4: Beam design calculation parameters

Beam	b (mm)	h (mm)	d (mm)	f_c (MPa)	f_y (MPa)	A_s (mm^2)
G1-BM1	150	150	112	30	420	157.08
G1-BM2	150	150	111	30	420	226.194
G1-BM3	150	150	111	30	420	339.291
G2-BM1	150	150	112	30	1250	157.08
G2-BM2	150	150	111	30	1250	226.194
G2-BM3	150	150	111	30	1250	339.291

4.4.4.3 Preparation of beams

A total of 6 beams were prepared; 3 group 1 beams reinforced with steel bars and 3 group 2 beams reinforced with GFRP bars. Wooden and steel mould were used for casting the beams as shown in Figure 4.10a. Oil was rubbed on the inner surface of the moulds to enable easy exit of the beams after setting. The reinforcement cages were inserted into the moulds with spacer attached to achieve the concrete cover of 25mm. Concrete was poured into the moulds and compacted using a rod to remove entrained air. The top of the beams were levelled using spatula. The beams were removed from the moulds after 24 hours and inserted into curing tank containing water at a temperature of 20±2°C. After 28days curing the beams were ready for testing.

(a) Beam moulds (b) Oiling the inner surface of moulds (c) Reinforcement cages

Figure 4.10: Preparation of beam moulds before concrete casting

(a) Beam moulds with reinforcement cages (b) Placement of mixed concrete

Figure 4.11: Casting of beam specimens

 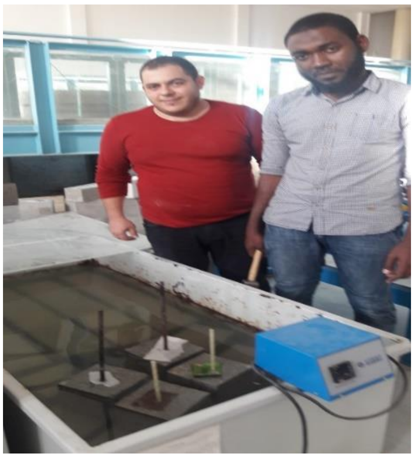

(a) Exiting of beams from moulds 24 hours (b) Beam specimens in curing tank

Figure 4.12: Curing of beam specimens

4.4.4.4 Four point bending test

The four point bending test was done in the KKTC Chambers of Civil Engineers laboratory and performed according to British standard (BS EN 12390-5).

The beams were placed in the automatic flexural testing machine (UTC-4000) with the supports positioned at 150mm from the both ends of the beams. The effective span of the beams were 450mm. the loading rollers was positioned at the top at 300mm from both ends of the beams. The loading setup and beam dimension is shown in Figure 4.13.

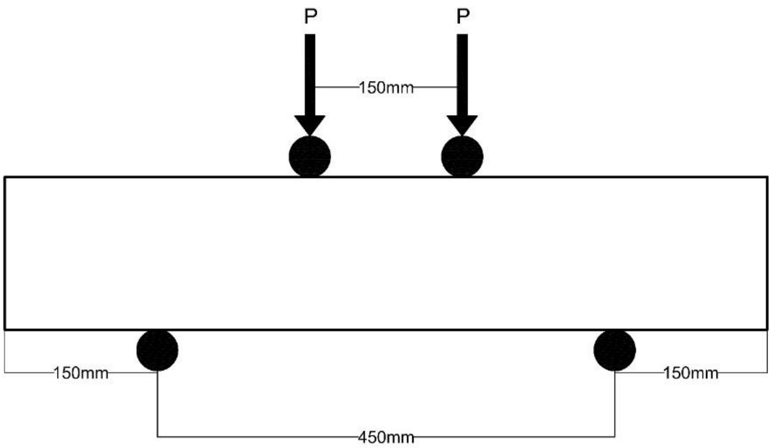

Figure 4.13: Diagram of loading arrangement of beams in flexural machine

The flexural testing machine has a loading capacity of 200kN. The load was applied until failure at a constant pace rate of 0.05MPa/s. Flexural strength of the beams can be computed using the equation below;

$$f_{cf} = \frac{F \times I}{d_1 \times d_2^2} \tag{12}$$

Where f_{cf} is the flexural strength, F is the maximum load, I is the distance between supporting rollers, d_1 and d_2 are the lateral dimensions of the specimen.

Figure 4.14: Loading setup of beams

CHAPTER 5

FINITE ELEMENT ANALYSIS (ABAQUS)

5.1 General

Several methods have been adopted in the past to determine the behavior of concrete. Experimental method has and will always be the preferred method of determining how reinforced concrete structures when subjected to loading behave due to its accuracy but it is costly and time consuming.

Finite element analysis has been used till today and is regarded as an excellent tool to solve problems in engineering. The FEA results visualizes the deformation of RC structures and also shows the stress and strain distribution and displacement respectively. Recently, many finite element analysis software have been created and is continuously used in analysing RC structures.

5.2 Modelling of beam specimens

A vast number of elements exists in ABAQUS which are used in solving numerous engineering problems. Examples of such elements includes C3D8R, C3D8I, J4R, T2D2 etc. these unique names identifies the aspects of each element.

5.2.1 Concrete

3D models were used to model the reinforced concrete beams. An eight nodes linear brick element with reduced integration (C3D8R) was adopted for the 3D models to model the concrete mass. This model consists of 8 nodes and each node having 3 degree of freedom. This type of element is able to show crushing, cracking and plastic deformation.

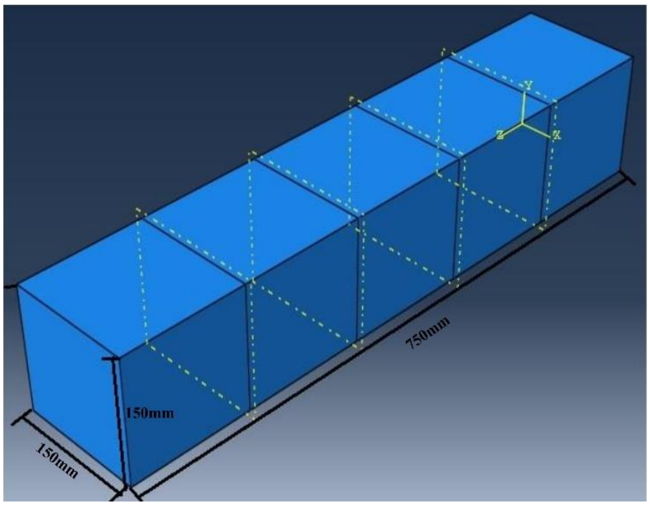

Figure 5.1: Sample of beam model used

5.2.2 Reinforcement

3D truss elements were used to model the reinforcement bars. A 3D two node linear truss element (T3D2) was adopted in the 3D models. A truss element is a slender long structural member which transmits axial forces only. Excellent bond between reinforcement bar and concrete is assumed because the GFRP and steel bars are embedded into the concrete element.

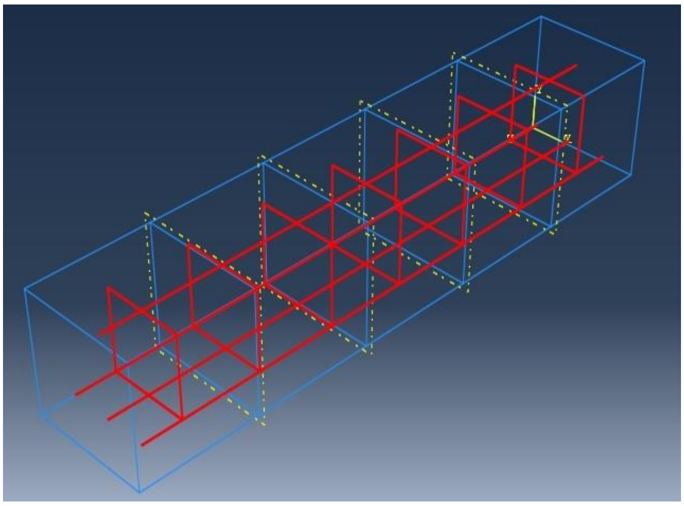

Figure 5.2: Sample of reinforcement cage embedded in the RC beam

5.3 Material Properties

All materials used in the analysis are defined as follows. The definition of the materials contain all the necessary material behaviours such as elastic material behaviour in a linear static stress analysis.

5.3.1 Concrete

The behaviour of concrete in compression and tension is different which makes the modelling to determine the concrete behaviour a difficult task.

Table 5.1: Material properties of concrete

Material properties		Values
Density		2400 kg/m^3
Elastic	Young's modulus	25384.9MPa
	Poisson ratio	0.15

The concrete damage plasticity (CDP) approach is adopted for the concrete modelling in this study. This approach make use of 4 parameters namely, compression hardening, tension stiffening, compression and tension damage. The stress strain relationship of these parameters is shown in appendix 3.

5.3.2 Steel bar

The steel bars were modelled as a perfectly elastic material. The elastic behaviour parameters are inserted respectively.

Table 5.2: Material properties of steel bar used

Material properties		**Values**
Elastic	Young's modulus	200GPa
	Poisson's ratio	0.3

5.3.3 GFRP bar

GFRP bars behave linearly until failure without yielding. They were modelled as a linear elastic material in ABAQUS. The elastic behaviour parameters are defined and the plastic behaviour parameters also.

Table 5.2: Material properties of GFRP bar used

Material properties		**Values**
Elastic	Young's modulus	55000MPa
	Poisson's ratio	0.21
Plastic	Yield stress	1250MPa
	Plastic strain	0.023

5.4 Loading and Boundary Conditions

Four point bending test was performed on the beams and load was applied on the model the same way it was on the experimental work. Displacement type loading was used and the displacement of 20mm was adopted. The beam was modelled as a simple beam just as in the experimental work. The supports are defined as pin and roller in the boundary condition option.

CHAPTER 6

RESULTS AND DISCUSSIONS

6.1 General

This chapter contains the detailed observations experienced during the tensile test, pull-out test and flexural test. The main objectives of the study was to determine the bond behaviour and flexural behaviour of steel and GFRP in RC members. Concrete of the same strength was used for the whole work and comparison was done between the ultimate load capacity of each specimen using different reinforcement materials.

6.2 Tensile Behaviour

The tensile test results of steel bars is shown in Table 6.1. Table 6.2 compared the properties of GFRP bars used in this experimental work and in previous experimental works.

Table 6.1: Mechanical properties of steel bars

Bar type	Diameter	Ultimate stress (MPa)	Modulus of elasticity (GPa)	% Elongation
Steel	8	567	210	17.4
	10	588	208	21.3
	12	705	210	14.5

Table 6.2: Mechanical properties of GFRP bars

Reference	Diameter (mm)	Ultimate stress (MPa)	Modulus of elasticity (GPa)	% Elongation
Liana composite*	8 10 12	1250	55	2.27
(Abdulsalam et al., 2018)	15.9	744	40.6	1.77
(Özkal et al., 2018)	9	918	49.9	1.84
(Johnson, 2009)	8 12	1374 1160	59.99 60.19	2.06 1.77
(Shin et al., 2009)	13	690	41	1.68
(Micelli & Nanni, 2004)	12	924	42.57	2.17
(Balendran et al., 2004)	8	1150	4700	2.45

*as provided by manufacturer

The tensile strength of the GFRP bars were unable to be determined due to certain encountered problems, which are;

- The total length of specimen to be used according to the standard was longer than maximum length of the tensile testing machine (UTM-6001).
- I tried using polyester adhesive but i experienced slippage between the GFRP bar and the hardened adhesive as shown in Figure 6.1
- According to the ASTM standard (D7205/D7205M-06), cement grout is the recommended filler material but i also used epoxy adhesive in the following trial

which is also an alternative material according to the standard and recent studies. I experienced slippage between the epoxy and the steel tube. It is shown in Figure 6.2.

Figure 6.1: Slippage between the GFRP bar and hardened polyester adhesive

Figure 6.2: Slippage between the hardened epoxy and steel tube

6.2 Bond Behaviour

The Table 6.3 gives a summary of the various configurations and experimental results of the pull-out test specimens.

Table 6.3: Summary of pull-out test results

Specimen	f'_c (MPa)	Bar diameter (mm)	Bar type	Embedded length (mm)	P_u (kN)	τ_{max} (MPa)	Failure mode*
S1	30	10	Steel	125	22.1	5.6	BP
S2	30	10	Steel	125	22.3	5.7	BP
G1	30	10	GFRP	125	25.9	6.6	CS
G2	30	10	GFRP	125	31.7	8.1	CS

*BP – Bar pull-out, CS – Concrete splitting

A total of 4 specimens where used to test the bond behaviour of steel and GFRP. All specimens where tested after 28 days curing. Specimens S1 and S2 where containing steel bars, both specimens failed due to bar pull-out from the concrete cube because of slippage between the steel bar and concrete as seen in Figure 6.1 and 6.2, this is as a result of weak bonding. Specimens G1 and G2 where containing GFRP bars, both the specimens failed due to concrete splitting as seen in Figure 6.3 and 6.4. This is as a result of excellent bond between the GFRP bar and concrete. Both the steel and GFRP are ribbed bars which are expected to bond well with concrete because of the nature of the surface.

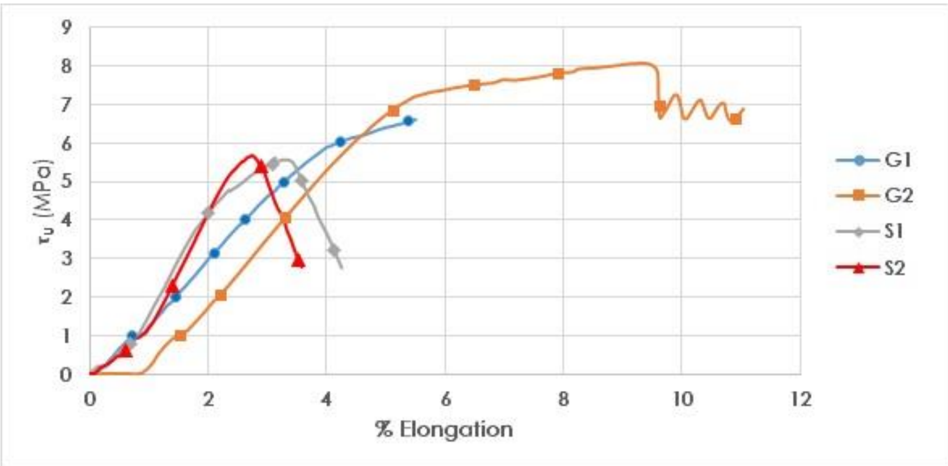

Figure 6.3: Comparison of maximum bond strength of pull-out specimens

Figure 6.4: S1 & S2 specimen failure mode

Figure 6.5: G1 specimen failure

Figure 6.6: G2 Specimen Failure

6.3 Flexural Behaviour

6.3.1 Ultimate load capacity

G1-BM1 & G2-BM1

The load was applied to the beams until failure. Beam G1-BM1 has an ultimate load of 103.64kN, the load at which the cracking start was 55kN while beam G2-BM1 has an ultimate load of 88.5kN and the first crack load was 35kN. Wide cracks where observed at the mid span of the beam G1-BM1. Beam G1-BM1 reinforced with steel bars withstood more load when compared to beam G2-BM2 reinforced with GFRP bars with a difference of 17%. The cracking load appeared to be much lower in beam G2-BM1 than in G1-BM1 which is due to the brittleness of the GFRP bar.

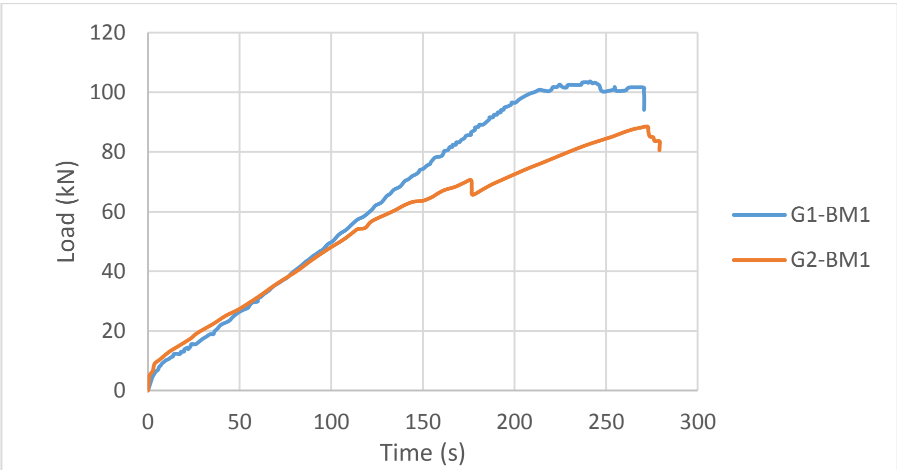

Figure 6.7: Ultimate load capacity comparison of G1-BM1 & G2-BM1 beam

G1-BM2 & G2-BM2

The load was applied to the beams until failure. G1-BM2 beam has an ultimate load capacity of 107.17kN and the first crack load was 94kN but G2-BM2 exhibits an ultimate load capacity of 102.06kN and the first crack load was 51kN. G1-BM2 (steel) withstood a little higher load than G2-BM2 (GFRP) with a difference of 5%. The first crack load of G2-BM2 was much lower than that of G1-BM2 because of the brittleness behaviour of GFRP bar.

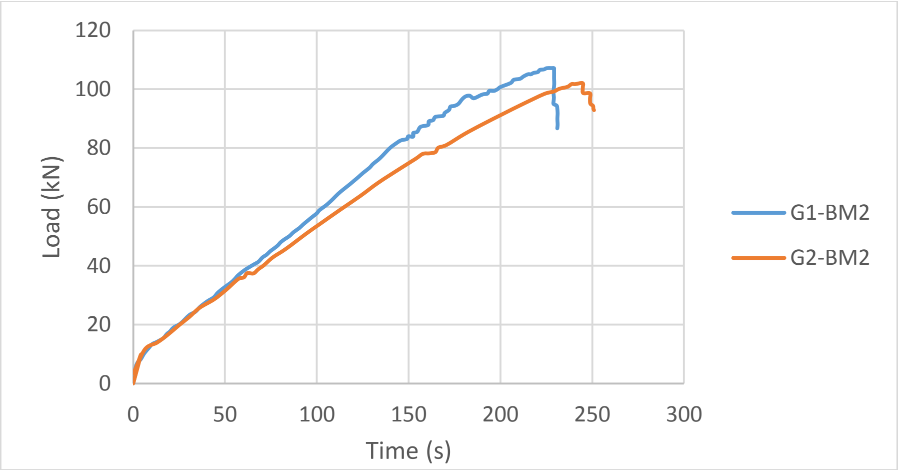

Figure 6.8: Ultimate load capacity comparison of G1-BM2 & G2-BM2 beam

G1-BM3 & G2-BM3

The load was applied to the beams until failure. G1-BM3 beam has an ultimate load capacity of 152.87kN and the first crack load was 134kN but G2-BM3 beam has an ultimate load capacity of 114.40kN and the first crack load was 63kN. G1-BM3 (steel) withstood a much higher load than G2-BM3 (GFRP) with a difference of 33.6%. The first crack load of G2-BM3 was also lower than that of G1-BM3 due to the nature of the GFRP bar.

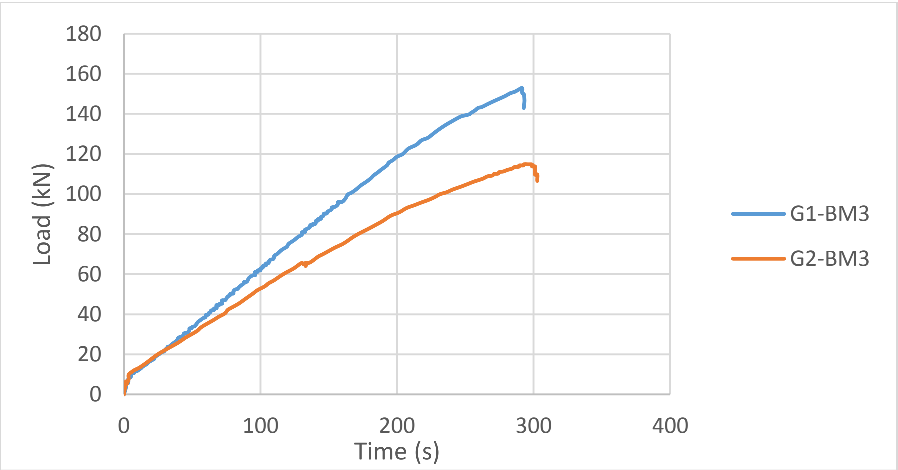

Figure 6.9: Ultimate load capacity comparison of G1-BM3 & G2-BM3 beam

6.3.2 Flexural strength

The flexural strength was computed according to BS EN 12390-5. The specimens have dimension of 750x150x150mm and tested after 28days curing to determine and compare the flexural strength of GFRP and steel reinforced concrete beams. The results are shown in Figure 6.4, 6.5, 6.6 and Table 6.2.

Table 6.4: Flexural strength of beam specimens

Specimen	f_{cf} (MPa)
G1-BM1	13.8
G1-BM2	14.3
G1-BM3	20.4
G2-BM1	11.8
G2-BM2	13.6
G2-BM3	15.3

6.3.3 Failure mode

G1-BM1 & G2-BM1

G1-BM1 beam exhibits a flexural cracks mid span of the beam which propagates from the extreme tension zone to almost the top of the beam and another faint crack is experienced from one support that propagates to the top of the beam with concrete crushing at the compression zone as shown in Figure 6.8. The G2-BM1 beam experienced only flexural cracks that propagates from the tension zone to the compression zone and crushing of concrete is also experienced as shown in Figure 6.9. G1-BM1 exhibits a diagonal compression failure while G2-BM1 exhibits a flexural failure.

Figure 6.10: Failure mode in beam G1-BM1

Figure 6.11: Failure mode in beam G2-BM1

G1-BM2 & G2-BM2

G1-BM2 beam consists of a revealing crack at one of the support and a faint crack at the other support, the crack propagates from the bottom to the top of the beam. No revealing flexural cracks were observed. G2-BM2 consists of few flexural cracks and some diagonal cracks at one support that propagates to the top of the beam with concrete crushing. G1-BM2 and G2-BM2 both exhibits diagonal tension failure.

Figure 6.12: Failure mode in beam G1-BM2

Figure 6.13: Failure mode in beam G2-BM2

G1-BM3 & G2-BM3

G1-BM3 consists of a faint flexural crack and some diagonal cracks at one of the supports which propagates from the bottom to the extreme top of the beam. G2-BM3 consists of flexural cracks and diagonal cracks at each of the supports that propagates from the bottom to the top of the beam. G1-BM3 exhibit a diagonal tension failure while G2-BM3 exhibits a diagonal compression failure.

Figure 6.14: Failure mode in beam G1-BM3

Figure 6.15: Failure mode in beam G2-BM3

6.3.4 Crack width

Crack width is one of the essential parameters that determines the aesthetics and performance of RC members. Crack width is controlled due to corrosion of steel. Crack width of 0.5mm and 0.7mm is permitted according to the ACI 440.1R-15. The crack width results are compared with the computed maximum crack width from the equation provided by the ACI code. The Table 6.3 shows the results of the crack width of the beams measured with a micrometre.

Table 6.5: Crack width of beam specimens

Specimen	w_{max} (mm)	w (mm)
G1-BM1	0.3	4.5
G1-BM2	0.35	2
G1-BM3	0.25	0.7
G2-BM1	2.5	2
G2-BM2	2.4	3
G2-BM3	1.6	4

Crack width of the GFRP reinforced concrete beams are found to be bigger than that of steel reinforced concrete beams which was expected except for G1-BM1. Some of the crack width are acceptable since it is within the acceptable limit as proposed by the American Concrete Institute, (2015). It can be observed that the crack widths of the steel reinforced concrete beam decreases as the reinforcement ratio increases but the crack widths of the GFRP reinforced concrete beams seems unpredictable. It is observed that the crack width is independent of the reinforcement ratio.

6.3.5 Summary of flexural behaviour results

The overall results of the parameters tested on the flexural behaviour of the beam specimens is summarized in the Table 6.6 below.

Table 6.6: Experimental flexural test results

Specimen	Bar type	ρ (%)	First crack load	P_u (kN)	w_{max} (mm)	w (mm)	f_{cf} (MPa)	Failure mode*
G1-BM1	Steel	1	55	103.64	0.3	0.7	13.8	DC
G1-BM2	Steel	1.4	94	107.17	0.35	0.3	14.3	DT
G1-BM3	Steel	2.1	134	152.87	0.25	0.15	20.4	DT
G2-BM1	GFRP	1	35	88.5	2.5	0.6	11.8	FF
G2-BM2	GFRP	1.4	51	102.06	2.4	0.4	13.6	DT
G2-BM3	GFRP	2.1	63	114.48	1.6	0.6	15.3	DC

*DC – Diagonal compression failure, DT – Diagonal tension failure, FF – Flexural failure

6.4 Finite Element Analysis Results

6.4.1 Ultimate load capacity and failure modes

Finite element analysis was done to see how the experimental results agrees with the ABAQUS results regarding the ultimate load and failure modes of the beams.

Table 6.7: Summary of FEA flexural results

Specimen	**Bar type**	**ρ (%)**	**P_u (kN)**	**f_{cf} (MPa)**	**Failure mode***
G1-BM1	Steel	1	89.34	11.9	DC
G1-BM2	Steel	1.4	97.49	13	DC
G1-BM3	Steel	2.1	106.57	14.2	DC
G2-BM1	GFRP	1	63.48	8.5	DC
G2-BM2	GFRP	1.4	69.68	9.3	DC
G2-BM3	GFRP	2.1	78.86	10.5	DC

*DC – Diagonal compression

G1-BM1 & G2-BM1

The ultimate load capacity of the G1-BM1 was 89.34kN which is higher than that of G2-BM1 which was 63.48kN with a difference of 40.7%. G1-BM1 have some few small flexural cracks around the tension zone with diagonal cracks that propagate from the bottom to the top of the beam. The G2-BM1 exhibits a diagonal cracks from the point of support to the extreme top of the beam with more flexural cracks mid span of the beam. G1-BM1 and G2-BM2 both exhibits diagonal compression failure.

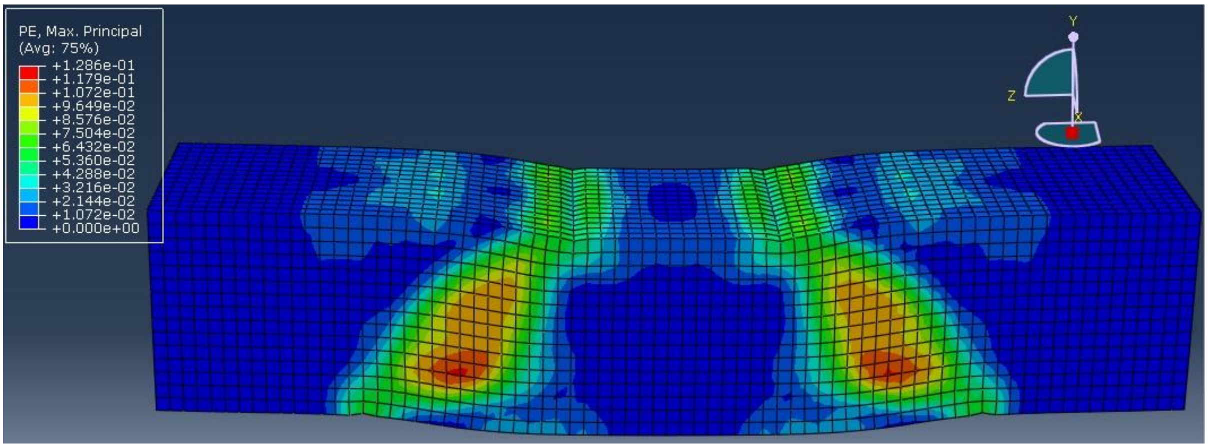

Figure 6.16: FEA failure mode of G1-BM1

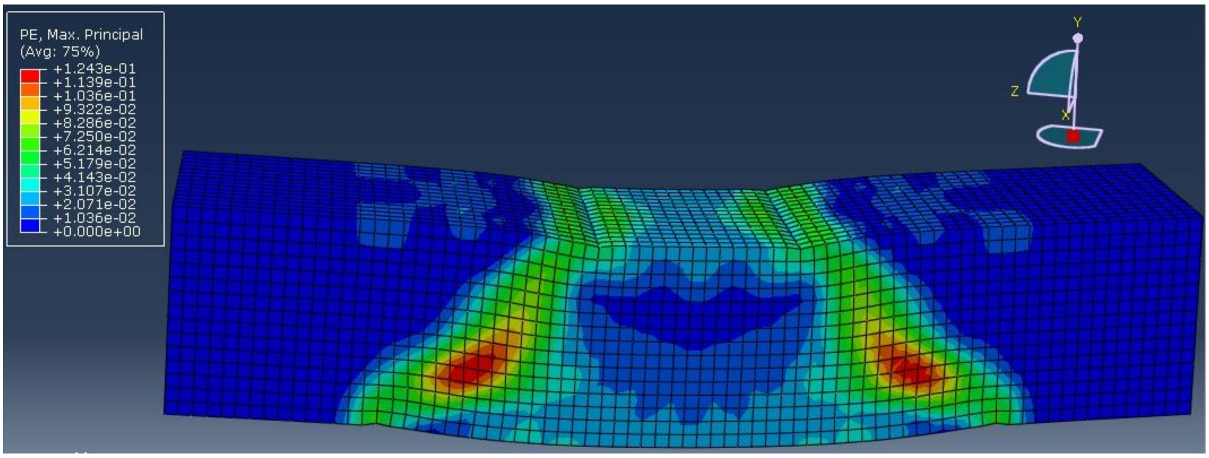

Figure 6.17: FEA failure mode of G2-BM1

G1-BM2 & G2-BM2

The ultimate load capacity of the G1-BM2 was 97.49kN which is higher than that of G2-BM2 which was 69.68kN with a difference of 39.7%. Diagonal cracks can be observed in G1-BM2 that moves from the support point to top of the beam. In G2-BM2, even though diagonal cracks exists at support points that moves to extreme compression zone, more flexural cracks are also observed. G1-BM2 and G2-BM2 both exhibits diagonal compression failure.

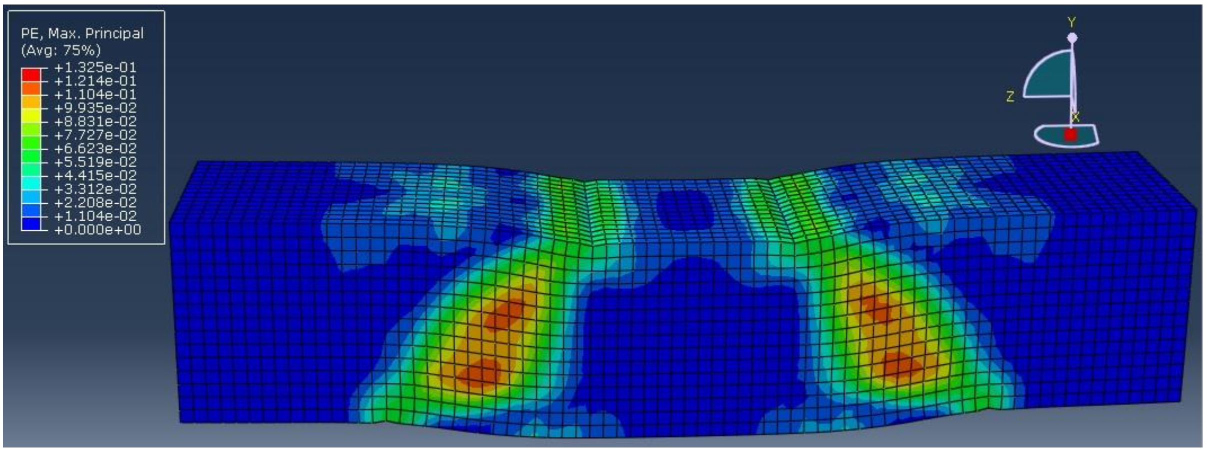

Figure 6.18: FEA failure mode of G1-BM2

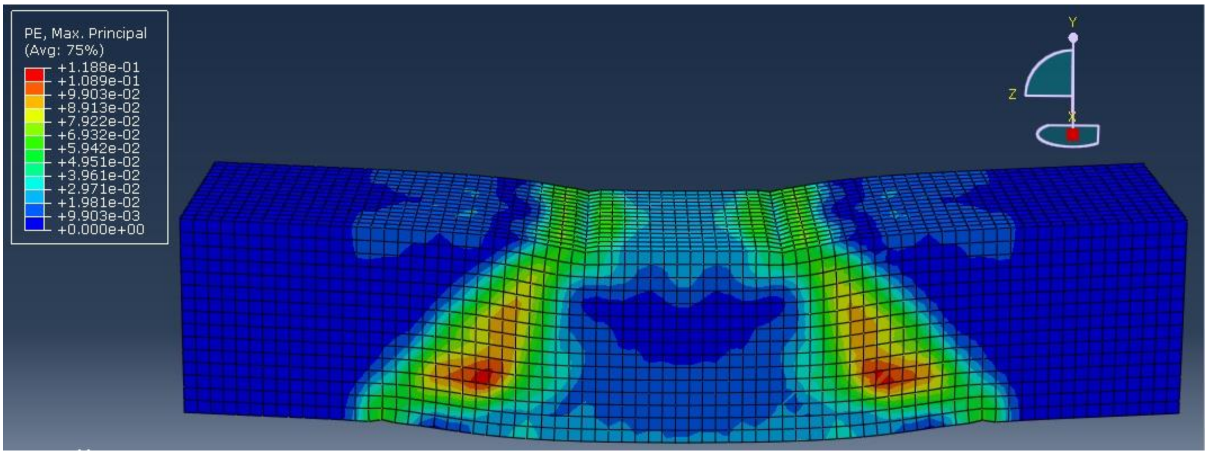

Figure 6.19: FEA failure mode of G2-BM2

G1-BM3 & G2-BM3

The ultimate load capacity of the G1-BM3 was 106.57kN which is much higher that of G2-BM3 which was 78.86kN with a difference of 35.1%. G1-BM3 contains diagonal cracks which moves from the support to the compression zone. G2-BM3 exhibits diagonal cracks but with flexural cracks also but not as much as G2-BM1 and G2-BM2 due to higher reinforcement ratio. G1-BM3 and G2-BM3 both exhibits diagonal compression failure.

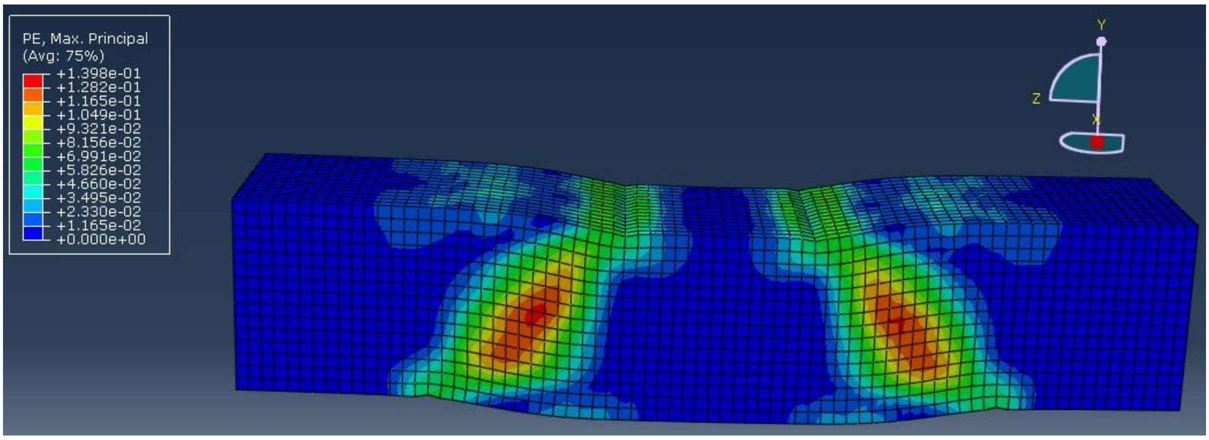

Figure 6.20: FEA failure mode of G1-BM3

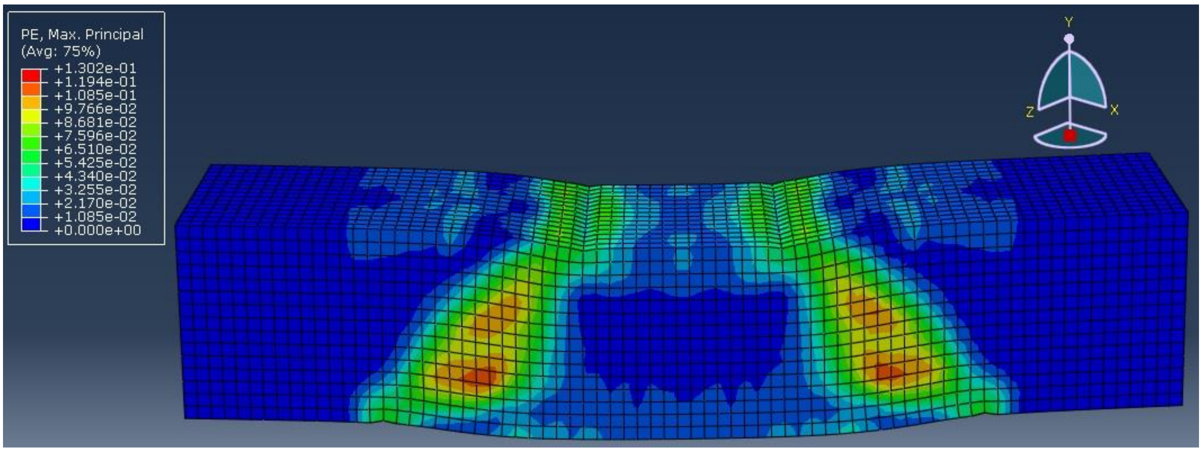

Figure 6.21: FEA failure mode of G1-BM3

6.5 Experimental and FEA Results Comparison

G1-BM1 & G2-BM1

It can be observed from the both experimental and FEA results that ultimate load capacity of the G1-BM1 beam is significantly higher than G2-BM1 beam. The experimental ultimate load capacity result for the G1-BM1 is 16% higher than the FEA result, however, it is 39.4% higher than the FEA result for the G2-BM1. The experimental and FEA failure mode experienced in both beams were generally shear failures.

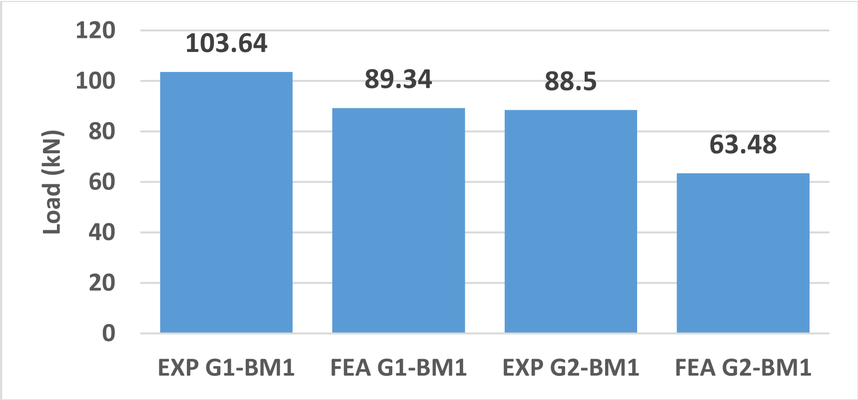

Figure 6.22: Comparison of FEA and experimental result for G1-BM1 & G2-BM1

G1-BM2 & G2-BM2

It can also be observed from the both experimental and FEA results that ultimate load capacity of the G1-BM2 beam is significantly higher than G2-BM2 beam. The experimental ultimate load capacity result for the G1-BM1 is 9.9% higher than the FEA result, however, it is 46.5% higher than the FEA result for the G2-BM2. The experimental and FEA failure modes exhibited by the beams were generally shear failures

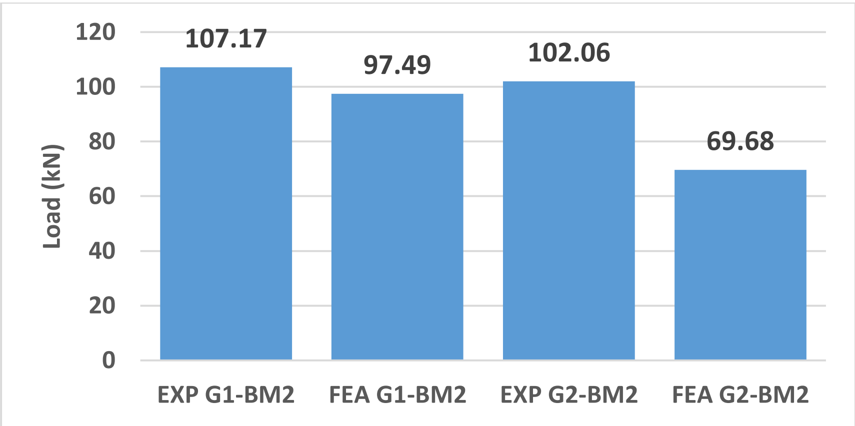

Figure 6.23: Comparison of FEA and experimental result for G1-BM2 & G2-BM2

G1-BM3 & G2-BM3

It can also be seen from the both experimental and FEA results that ultimate load capacity of the G1-BM3 beam is significantly higher than G2-BM3 beam. The experimental ultimate load capacity result for the G1-BM1 is 43.4% higher than the FEA result, however, it is 45.2% higher than the FEA result for the G2-BM3. The failure modes experienced in the experimental and FEA results were generally shear failures.

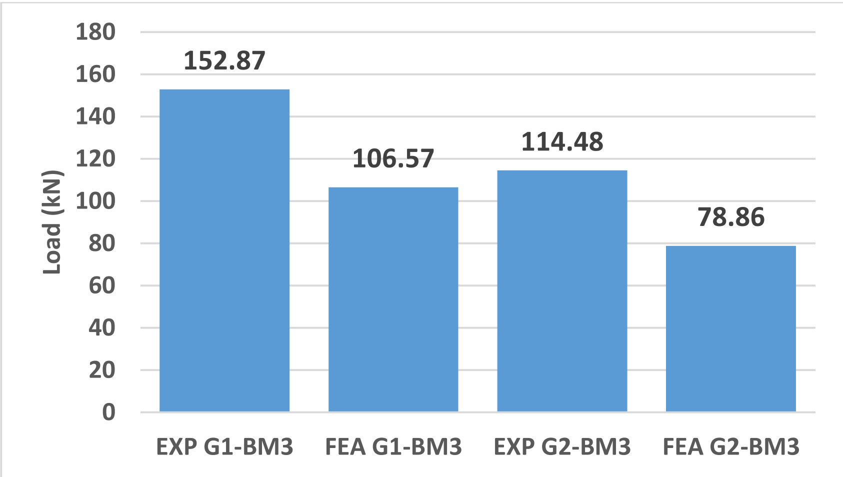

Figure 6.24: Comparison of FEA and experimental result for G1-BM3 & G2-BM3

6.6 Cost Comparison

The summary of the weight and cost of steel and GFRP bars with respect to 1 running meter and the standard length of 12m is stated in Table 6.8. It can be seen that regarding the weight of the reinforcement bars, the weight of steel bars are significantly higher than that of GFRP bars. But in terms of the cost, it can be seen that the cost of GFRP bars are higher than that of steel bars but it can be seen that the price gap between the steel bars reduces as the diameter of the reinforcement bars increases. The Φ8 GFRP bar cost is 41.2% more than the corresponding steel bar, the Φ10 GFRP bar cost is 29.6% more than the corresponding steel bar, also the Φ 12 GFRP bar costs is 17.6% more than the corresponding steel bar.

Table 6.8: Cost of reinforcement bars

Item		Kg/m	Kg/12m	Price($)/m	Price($)/12m
Steel	Φ8	0.395	4.74	0.227	2.72
	Φ10	0.616	7.392	0.355	4.26
	Φ12	0.888	10.656	0.51	6.12
GFRP	Φ8	0.072	0.864	0.32	3.84
	Φ10	0.11	1.32	0.46	5.52
	Φ12	0.184	2.208	0.60	7.2

The total cost of the reinforcement cages of each beam specimen is shown in Table 6.9. It can be observed that the cost of steel reinforcement cages is significantly lower than GFRP reinforcement cages. The difference ranges from 11% to 14%. But the steel reinforcement in the beam were cheaper and able to resist more loads than the GFRP reinforced beam with percentage differences of 17% for BM1, 5% for BM2 and 33% for BM3, which significantly shows that for the GFRP reinforced beams needs to be overly reinforced for it carry the corresponding load a steel reinforced beam could carry. Also according to Berg et al, (2006), the material cost of GFRP reinforced members are significantly higher than the steel reinforced materials, but the benefits of using GFRP includes low labour expenses, low transport expenses, little or no maintenance cost due to corrosion resistance and longer life span.

Table 6.9: Total cost of reinforcement cage of specimens

Specimen		Bottom reinforcement	Top reinforcement	Stirrups (steel)	Total ($)
G1-BM1	Diameter	Φ10	Φ8	Φ8	1.45
	Length (m)	1.4	0.7	3.5	
	Price ($)	0.497	0.159	0.795	
G1-BM2	Diameter	Φ12	Φ8	Φ8	1.67
	Length (m)	1.4	0.7	3.5	
	Price ($)	0.714	0.159	0.795	
G1-BM3	Diameter	Φ12	Φ8	Φ8	2.03
	Length (m)	2.1	0.7	3.5	
	Price ($)	1.071	0.159	0.795	
G2-BM1	Diameter	Φ10	Φ8	Φ8	1.66
	Length (m)	1.4	0.7	3.5	
	Price ($)	0.644	0.224	0.795	
G2-BM2	Diameter	Φ12	Φ8	Φ8	1.86
	Length (m)	1.4	0.7	3.5	
	Price ($)	0.84	0.224	0.795	
G2-BM3	Diameter	Φ12	Φ8	Φ8	2.28
	Length (m)	2.1	0.7	3.5	
	Price ($)	1.26	0.224	0.795	

CHAPTER 7

CONCLUSIONS AND RECOMMENDATIONS

The summary of the experimental and analytical result findings are presented in this chapter.

- The tensile strength of GFRP bars are significantly higher when compared to that of steel bars but the GFRP specimen should be well prepared according to standard in order to achieve the satisfactory result.
- The average tensile strength of the GFRP bars is about 65% higher than that of steel bars.
- The bond strength was determined using pull-out test and the specimen G1 and G2 containing GFRP bar has higher average maximum bond strength than specimen S1 and S2 containing steel bar with about 30%.
- The bond strength of the GFRP bars mainly rely upon the ribs and the inner cores of the reinforcing bars.
- The failure mode of specimen S1 and S2 was bar pull-out, this is due to weak bonding causing slippage of the steel bar from the concrete although the surface is ribbed which should improve its adhesion to concrete and provide resistance while specimen G1 and G2 failed due to concrete splitting signifying excellent bonding between helically ribbed GFRP bar and concrete.
- The ultimate load capacity of steel reinforced beams is higher than GFRP reinforced beams both having the same reinforcement ratios.
- The ultimate load capacity of group 1 beams when compared to group 2 beams having reinforcement ratio of 1 increased by 17%, with reinforcement ratio of 1.4 it increased by 5% and with reinforcement ratio of 2.1 it increased by 33.6%.
- Similarly, the flexural strength of the group 1 beams is higher than that of group 2 beam, this is due to the low elastic modulus of GFRP bar.
- The beam specimens are limited to short spans which usually failed by shear failures at ultimate load.

- The failure modes observed in group 1 beams are generally shear failures but group 2 beams also exhibits shear failures but with a lot of flexural cracks which is expected in GFRP reinforced beams due to its brittle nature.
- Crack width of some of the beam specimen are within the acceptable limit based on the maximum crack width equation proposed by the ACI 440.1R-15
- It is also observed that crack width of the GFRP reinforced beams are independent of the reinforcement ratio.
- It can also be observed that the FEA results closely agrees with the experimental results regarding the ultimate load capacity of group 1 beams being higher than group 2 beams.
- The failure mode experienced in the FEA results is more accurate than the experimental results due the smaller mesh size adopted for the beam models.
- The failure mode in the FEA result for group 1 beams were shear failures and group 2 beams were also shear failures with a lot of flexural cracks. It can be seen that it also closely agrees with the failure modes experienced in the experimental results.
- It can be observed that the flexural cracks experienced in the FEA results reduces as the reinforcement ratio increases.
- The price of the GFRP bar is higher than steel bar. The total cost of the steel reinforcement cages is significantly lower than the GFRP reinforcement cages and the difference varies from 11% to 14%.
- Although they have high initial cost but its ease of transport, little or no maintenance cost due to its non-corrosive nature still makes it to be considered as a good alternative material steel bars. Therefore considering the lifecycle cost, the GFRP bar can be said to be a better reinforcing material than steel.

Awareness should be raised regarding the use of GFRP bars as reinforcing materials since it is able to resist a considerable amount of applied load and also to avoid corrosion menace and high maintenance cost attributed to corrosion problem.

Use of cement grout as filler material between the steel tube and GFRP bar in preparation of tensile test specimen is highly recommended. A good epoxy adhesive material is recommended as alternative if cement grout unavailable.

REFERENCES

Abdalla, H. A. (2002). Evaluation of Deflection in Concrete Members Reinforced with Fibre Reinforced Polymer (FRP) Bars. *Composite Structures*, *56*, 63–71.

Abdulsalam, B., Farghaly, A., Gagné, R., Adel, E., Alam, P., & Benmokrane, B. (2018). Behaviour of concrete prisms reinforced by various types of glass fibre reinforced polymer (GFRP) bars. In *10th International Conference on Short and Medium Span Bridges* (Vol. 440, pp. 1–10). Quebec, Canada.

Ahmed, E. A., Benmokrane, B., & Sansfaçon, M. (2016). Design, Construction, and Performance of the La Chancelière Parking Garage's Concrete Flat Slabs Reinforced with GFRP Bars. *American Society of Civil Engineers*, 1–15.

American Concrete Institute. (2015). ACI 440.1R-15: Guide for the Design and Construction of Structural Concrete Reinforced with FRP Bars. *ASTM Book of Standards*.

Ashour, A. F. (2006). Flexural and shear capacities of concrete beams reinforced with GFRP bars. *Construction and Building Materials*, *20*(10), 1005–1015.

Aslan FRP. (2018a). Aslan 100 fiberglass rebar - Marine and Waterfront construction photos. Retrieved August 30, 2018, from http://aslanfrp.com/Aslan100/Aslan100_Waterfront-Marine.html

Aslan FRP. (2018b). Aslan 100 fiberglass rebar - MRI Room construction photos. Retrieved August 30, 2018, from http://aslanfrp.com/Aslan100/Aslan100_Hospital_MRI_Rooms.html

Balendran, R. V., Rana, T. M., Maqsood, T., & Tang, W. C. (2002). Application of FRP bars as reinforcement in civil engineering structures. *Structural Survey*, *20*(2), 62–72.

Balendran, R. V, Tang, W. E., Leung, H. Y., & Nadeem, A. (2004). Flexural Behaviour of Sand Coated Glass-Fibre Reinforced Polymer (GFRP) Bars in Concrete. In *Our World in Concrete & Structures* (p. 11). Singapore.

Barris, C., Torres, L., Baena, M., Pilakoutas, K., & Guadagnini, M. (2012). Serviceability Limit State of FRP RC Beams. *Advances in Structural Engineering*, *15*(4), 653–664.

Benmokrane, B., Theriault, M., Masmoudi, R., & Rizkalla, S. (1997). Effect of reinforcement ratio on concrete members reinforced with FRP bars. *SAMPE'97 Symposium*, 1–11.

Berg, A. C., Bank, L. C., Oliva, M. G., & Russell, J. S. (2006). Construction and cost analysis of an FRP reinforced concrete bridge deck. *Construction and Building Materials*, *20*(8), 515–526.

Bhatnagar, N., & Asija, N. (2016). Durability of high-performance ballistic composites. *Lightweight Ballistic Composites*, 231–283.

Birtel, V., & Mark, P. (2006). Parameterised Finite Element Modelling of RC Beam Shear Failure. In *Abaqus User's Conference* (pp. 95–108).

Bouzouaid, S., & Kriker, A. (2017). Nonlinear analysis of concrete beams strengthened by date palm fibers. *AIP Conference Proceedings*, *1814*.

British Standards. (2009). BS EN 12390-5 - Flexural Strength of Test Specimens. *British Standard Institutes*. https://doi.org/10.1515/bmte.1992.37.s1.137

Brown, J. (2014). *Glass Fibre Reinforced Polymer Bars in Concrete Compression*. *Airey Taylor Consulting*.

CAN/CSA-S6-06. (2010). Canadian Highway Bridge Design Code. *A National Standard of Canada Single*.

Chidananda, S. H., & Khadiranaikar, R. B. (2017). Flexural Behaviour of Concrete Beams Reinforced With GFRP Rebars. *International Journal of Advance Research, Ideas and Innovations in Technology*, *3*(5), 119–128.

Composites World. (2011). A Hidden Revolution: FRP Rebar Gains Strength. Retrieved August 30, 2018, from https://www.compositesworld.com/articles/a-hidden-revolution-frp-rebar-gains-strength

Devi, G. N. (2015). Fiber Reinforced Polymer Reinforcing Bars in Concrete Structures. *International Journal of Innovative Research in Science, Engineering and Technology Engineering and Technology*, *4*(6), 4832–4840.

Fico, R. (2008). *Limit States Sesign of Concrete Structures Reinforced with FRP Bars*. *Doctoral dissertation, University of Naples Federico II*. University of Naples Federico II.

George, V., & Parappattu, N. B. (2017). Comparative Study of GFRP Rebar and Steel Rebar used in Concrete Sections. *Global Research and Development Journal for Engineering*, *2*(6), 36–41.

Gökçekuş, H. (1994). KKTC Deki Taşocaklarının Görsel Çevre İle Yeraltısuyu Kaynakları Üzerindeki Etkileri. In *KKTC De Çevre Sorunları Sempozyumu*. Lefkoşa: Kıbrıs Türk Mühendis ve Mimar Odaları Birlığı.

Hibbitt, K. and S. I. (1992). ABAQUS: Theory Manual. *Notes*.

Hollaway, L. C. (2010). A review of the present and future utilisation of FRP composites in the civil infrastructure with reference to their important in-service properties. *Construction and Building Materials*, *24*(12), 2419–2445.

Jalil, A. M. A. (2014). Mechanical Properties of Glass Fiber Reinforced Polymer Bars After Exposure to Elevated Temperatures. *Masters Thesis, The University of Wisconsin – Milwaukee*, (December).

Japan Society of Civil Engineers. (1996). Recommendation For Design And Construction Of Concrete Structures Using Continuous Fiber Reinforcing Materials. *Concrete Engineering Series 23*, (1), 1–58.

Johnson, D. (2009). *Investigation of Glass Fibre Reinforced Polymer Reinforcing Bars as Internal Reinforcement for Concrete Structures*. *Masters Thesis, University of Toronto*.

Kheni, H. L., Satasiya, A. P., Balar, K. P., & Khokhar, P. R. (2016). GFRP Bars as a Substitution in Structure. *Global Research and Development Journal for Engineering*, *035*, 193–196.

Kocaoz, S., Samaranayake, V. A., & Nanni, A. (2005). Tensile characterization of glass FRP bars. *Composites Part B: Engineering*, *36*(2), 127–134.

Machida, A., & Uomoto, T. (1997). Recommendation for Design and Construction of Concrete Structures Using Continuous Fiber Reinforcing Material (Design). *Japan*

Society of Civil Engineers, 88.

Masmoudi, R., Benmoktane, B., & Chaallalt, O. (1995). Glass fibre reinforced plastic concrete structures rebars for. *Construction and Building Materials*, *9*(6), 353–364.

Masmoudi, R., Zaidi, A., & Gérard, P. (2005). Transverse Thermal Expansion of FRP Bars Embedded in Concrete. *Journal of Composites for Construction*, *9*(5), 377–387.

Mateenbar.com. (2018). History of FRP. Retrieved April 16, 2018, from http://www.mateenbar.com/history-of-frp/

Maurizio, G. (2010). Fibre Reinforced Polymers. Retrieved August 19, 2018, from http://mguadagnini.staff.shef.ac.uk/frp/frp.php

Micelli, F., & Nanni, A. (2004). Durability of FRP rods for concrete structures. *Construction and Building Materials*, *18*(7), 491–503.

Michael, C. B. (2002). *Corrosion Protection Service Life of Epoxy Coated Reinforcing Steel in Virginia Bridge Decks*. *Doctoral dissertation, Virginia Polytechnic Institute and State University*. Virginia Polytechnic Institute and State University.

NACE International. (2000). Lowe's Motor Speedway Bridge Collapse. Retrieved August 12, 2018, from https://www.nace.org/CORROSION-FAILURES-Lowes-Motor-Speedway-Bridge-Collapse.aspx

NACE International. (2013). Leo Frigo Memorial Bridge Failure. Retrieved August 12, 2018, from https://www.nace.org/Corrosion-Failure-Leo-Frigo-Memorial-Bridge-Failure.aspx

Naimi, S., & Celikag, M. (2014). Problems of Reinforced Concrete Building Construction in North Cyprus, (April 2010).

Nanni, A. (2000). FRP Reinforcement for Structures. In *Strucural Engineering Conference* (p. 5).

Nanni, A., & Gold, W. J. (1998). Strength Assessment of External FRP Reinforcement. *Concrete International*, *20*(6), 39–42.

Nilson, A. H., David, D., & Dolan, C. W. (2010). *Design of Concrete Structures*. *McGraw-*

Hill (14th ed.). Mc Graw Hill.

Özkal, F. M., Polat, M., Yağan, M., & Öztürk, M. O. (2018). Mechanical properties and bond strength degradation of GFRP and steel rebars at elevated temperatures. *Construction and Building Materials*, *184*(July), 45–57.

Rahmatian, A. (2014). *Static and Fatigue Behaviour of FRP-Reinforced Concrete Beams and a SHM System with Fiber Optic Sensors under Different Weathering Conditions*. Concordia University.

Rob, B. P., Leegwater, G., Worm, D., & Courage, W. (2012). Service Life and Life Cycle Cost Modelling of Cathodic Protection Systems. In *International Congress on Durability of Concrete*.

Saafi, M. (2002). Effect of Fire on FRP Reinforced Concrete Members. *Composite Structures*, *58*(1), 11–20.

Saenz, L. P. (1964). Discussion of "Equation for the stress-strain curve of concrete," by Desayi and Krishnan. *ACI Journal*, *61*(9).

Said, M. N. (2014). *Experimental Investigation and Behaviour of Reinforced Concrete Beams Strengthened With CFRP*. *Masters Thesis*. Near East University.

Saikia, B., Thomas, J., Ramaswamy, A., & Nanjunda Rao, K. S. (2005). Performance of Hybrid Rebars as Longitudinal Reinforcement in Normal Strength Concrete. *Materials and Structures/Materiaux et Constructions*, *38*(284), 857–864.

Salh, L. (2014). *Analysis and Behaviour of Structural Concrete Reinforced with Sustainable Materials*. *Masters Thesis, University of Liverpool*.

Shanour, A. S., Mahmoud, A. A., Adam, M. A., & Said, M. (2014). Experimental Investigation of Concrete Beams Reinforced with GFRP Bars. *International Journal of Civil Engineering and Technology*, *5*(11), 154–164.

Shin, S., Seo, D., & Han, B. (2009). Performance of Concrete Beams Reinforced with GFRP Bars. *Journal of Asian Architecture and Building Engineering*, *8*(1), 197–204.

Sonnenschein, R., Gajdosova, K., & Holly, I. (2016). FRP Composites and Their Using in the Construction of Bridges. *Procedia Engineering*, *161*, 477–482.

State Planning Organization. (2016). Building Construction and Parcel Statistics.

Stoner, J. G. (2015). Finite Element Modelling of GFRP Reinforced Concrete Beams. *Masters Thesis, University of Waterloo*.

Thippeswamy, H. K., Franco, J. M., & GangaRao, H. V. S. (1998). FRP Reinforcement in Bridge Deck. *Concrete International*, *20*(6).

TUF-BAR. (2018). TUF-BAR | Parking Garages Reinforced With Fiberglass. Retrieved August 28, 2018, from https://www.tuf-bar.com/application/parking-garages/

Wahalathantri, B.L. Thambiratnam, D. P., Chan, T. H. T., & Fawzia, S. (2011). A Material Model for Flexural Crack Simulation in Reinforced Concrete Elements Using ABAQUS. In *First International Conference on Engineering, Designing and Developing the Built Environment for Sustainable Wellbeing* (Vol. 46, pp. 260–264).

Wang, H., Zha, X., & Ye, J. (2009). Fire Resistance Performance of FRP Rebar Reinforced Concrete Columns. *International Journal of Concrete Structures and Materials*, *3*(2), 111–117.

Worner, V. J. (2015). *Use of Glass Fibre Reinforced Polymer (GFRP) Reinforcing Bars for Concrete Bridge Decks*. University of Canterbury.

Wu, W.-P. (1990). *Thermomechanical Properties of Fiber Reinforced Plastic (FRP) bars*.

APPENDICES

Appendix 1

Graphical results of the compression, tensile, flexural and pull-out tests

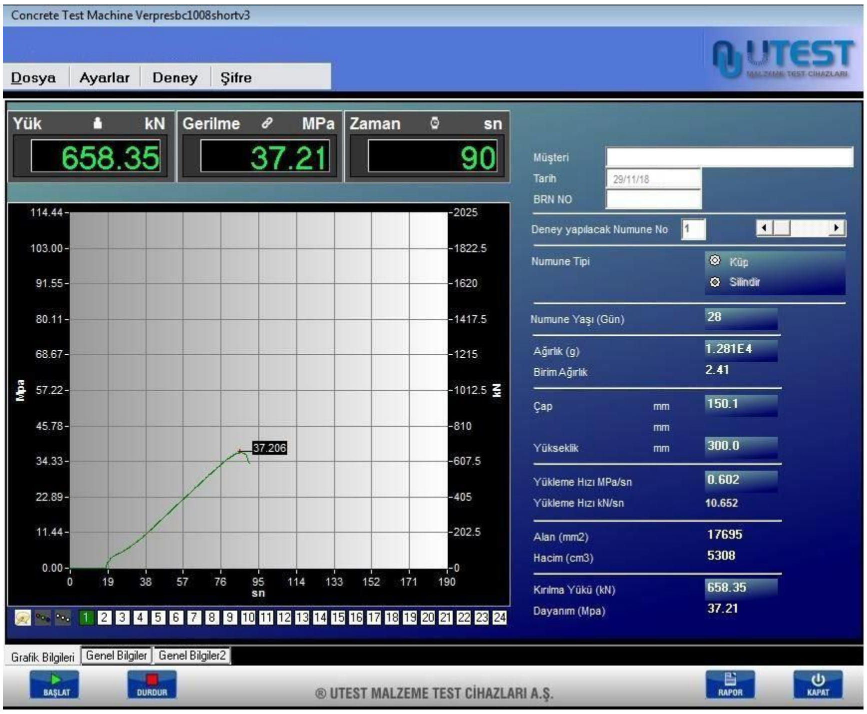

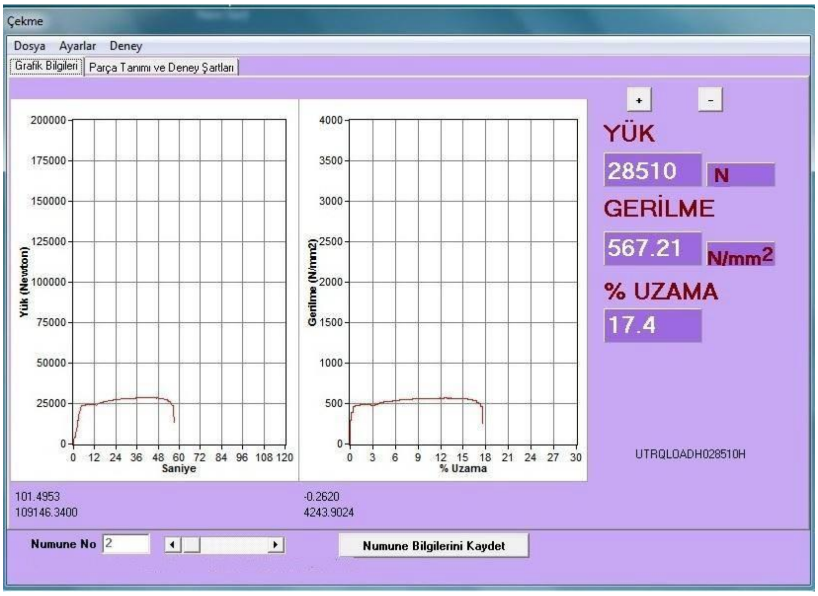
Çekme
Dosya Ayarlar Deney
Grafik Bilgileri
Parça Tanımı ve Deney Şartları
YÜK
28510
N
GERİLME
567.21
N/mm2
% UZAMA
17.4
Yük (Newton)
Saniye
Gerilme (N/mm2)
% Uzama
101.4953
109146.3400
-0.2620
4243.9024
UTRQLOADH028510H
Numune No
Numune Bilgilerini Kaydet

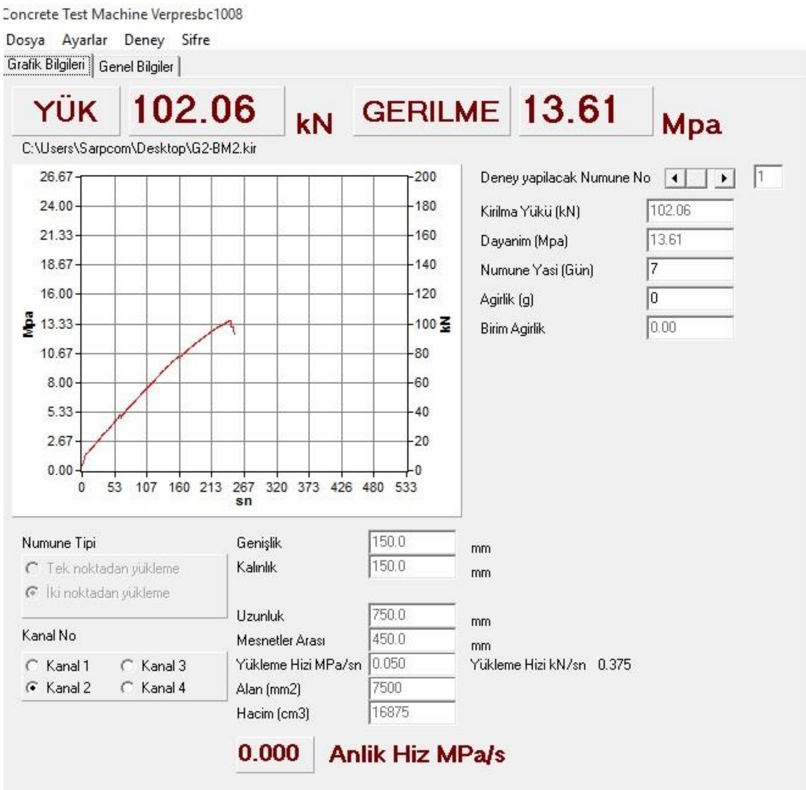
Concrete Test Machine Verpresbc1008
Dosya Ayarlar Deney Sifre
Grafik Bilgileri
Genel Bilgiler
YÜK
102.06
kN
GERILME
13.61
Mpa
C:\Users\Sarpcom\Desktop\G2-BM2.kir
Mpa
kN
sn
Deney yapilacak Numune No
Kirilma Yükü (kN) 102.06
Dayanim (Mpa) 13.61
Numune Yasi (Gün) 7
Agirlik (g) 0
Birim Agirlik 0.00
Numune Tipi
Tek noktadan yükleme
İki noktadan yükleme
Kanal No
Kanal 1
Kanal 2
Kanal 3
Kanal 4
Genişlik 150.0 mm
Kalınlık 150.0 mm
Uzunluk 750.0 mm
Mesnetler Arası 450.0 mm
Yükleme Hizi MPa/sn 0.050
Yükleme Hizi kN/sn 0.375
Alan (mm2) 7500
Hacim (cm3) 16875
0.000
Anlik Hiz MPa/s

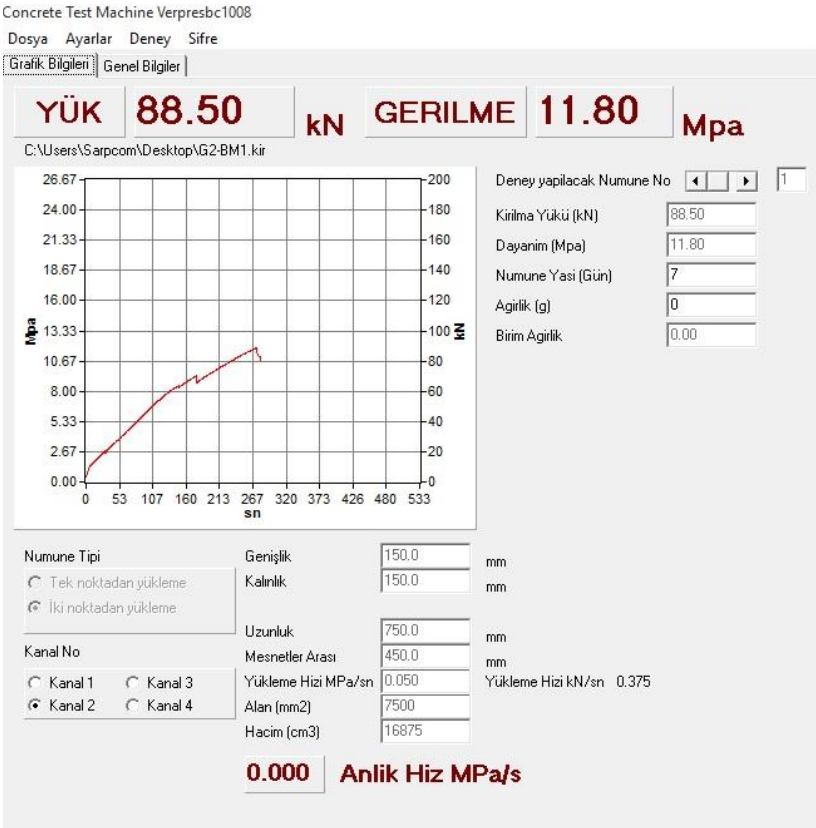
Concrete Test Machine Verpresbc1008
Dosya Ayarlar Deney Sifre
Grafik Bilgileri Genel Bilgiler
YÜK 88.50 kN GERILME 11.80 Mpa
C:\Users\Sarpcom\Desktop\G2-BM1.kir
Mpa
kN
sn
Deney yapilacak Numune No 1
Kirilma Yükü (kN) 88.50
Dayanim (Mpa) 11.80
Numune Yasi (Gün) 7
Agirlik (g) 0
Birim Agirlik 0.00
Numune Tipi
Tek noktadan yükleme
İki noktadan yükleme
Kanal No
Kanal 1 Kanal 3
Kanal 2 Kanal 4
Genişlik 150.0 mm
Kalınlık 150.0 mm
Uzunluk 750.0 mm
Mesnetler Arası 450.0 mm
Yükleme Hizi MPa/sn 0.050
Yükleme Hizi kN/sn 0.375
Alan (mm2) 7500
Hacim (cm3) 16875
0.000 Anlik Hiz MPa/s

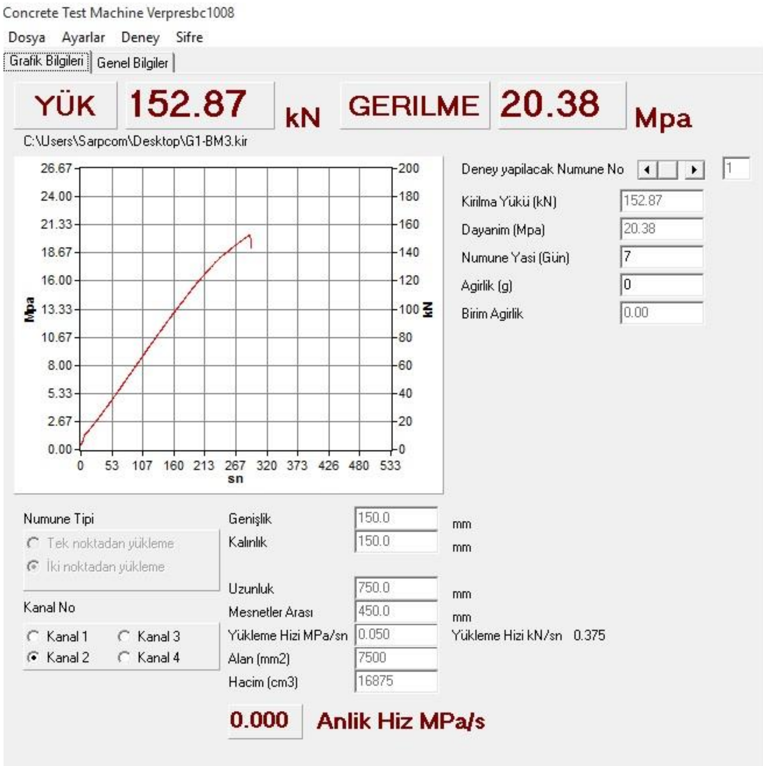
Concrete Test Machine Verpresbc1008
Dosya Ayarlar Deney Sifre
Grafik Bilgileri Genel Bilgiler
YÜK 152.87 kN GERILME 20.38 Mpa
C:\Users\Sarpcom\Desktop\G1-BM3.kir
Mpa
kN
sn
Deney yapilacak Numune No 1
Kirilma Yükü (kN) 152.87
Dayanim (Mpa) 20.38
Numune Yasi (Gün) 7
Agirlik (g) 0
Birim Agirlik 0.00
Numune Tipi
Tek noktadan yükleme
İki noktadan yükleme
Kanal No
Kanal 1 Kanal 3
Kanal 2 Kanal 4
Genişlik 150.0 mm
Kalınlık 150.0 mm
Uzunluk 750.0 mm
Mesnetler Arası 450.0 mm
Yükleme Hizi MPa/sn 0.050
Yükleme Hizi kN/sn 0.375
Alan (mm2) 7500
Hacim (cm3) 16875
0.000 Anlik Hiz MPa/s

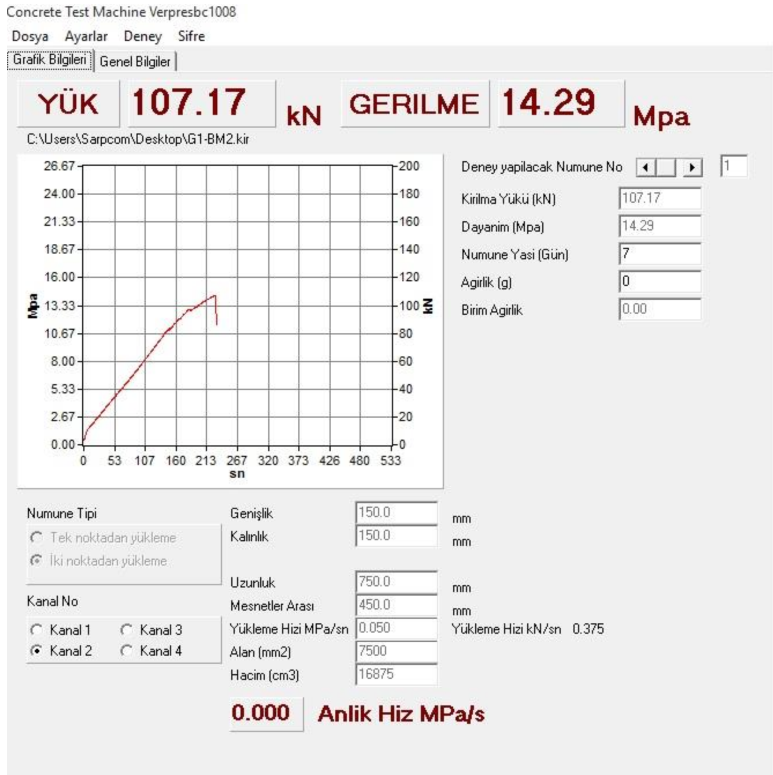
Concrete Test Machine Verpresbc1008
Dosya Ayarlar Deney Sifre
Grafik Bilgileri
Genel Bilgiler
YÜK
107.17
kN
GERILME
14.29
Mpa
C:\Users\Sarpcom\Desktop\G1-BM2.kir
Deney yapilacak Numune No
Kirilma Yükü (kN) 107.17
Dayanim (Mpa) 14.29
Numune Yasi (Gün) 7
Agirlik (g) 0
Birim Agirlik 0.00
Numune Tipi
Tek noktadan yükleme
İki noktadan yükleme
Kanal No
Kanal 1 Kanal 3
Kanal 2 Kanal 4
Genişlik 150.0 mm
Kalınlık 150.0 mm
Uzunluk 750.0 mm
Mesnetler Arası 450.0 mm
Yükleme Hizi MPa/sn 0.050
Yükleme Hizi kN/sn 0.375
Alan (mm2) 7500
Hacim (cm3) 16875
0.000
Anlik Hiz MPa/s

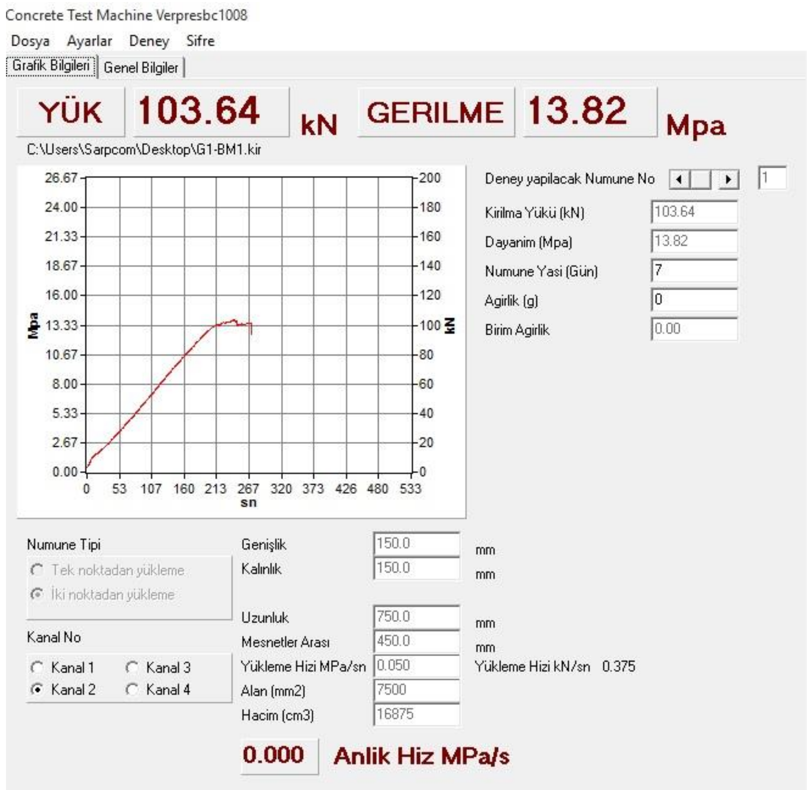
Concrete Test Machine Verpresbc1008
Dosya Ayarlar Deney Sifre
Grafik Bilgileri
Genel Bilgiler
YÜK
103.64
kN
GERILME
13.82
Mpa
C:\Users\Sarpcom\Desktop\G1-BM1.kir
Deney yapilacak Numune No
Kirilma Yükü (kN) 103.64
Dayanim (Mpa) 13.82
Numune Yasi (Gün) 7
Agirlik (g) 0
Birim Agirlik 0.00
Numune Tipi
Tek noktadan yükleme
İki noktadan yükleme
Kanal No
Kanal 1 Kanal 3
Kanal 2 Kanal 4
Genişlik 150.0 mm
Kalınlık 150.0 mm
Uzunluk 750.0 mm
Mesnetler Arası 450.0 mm
Yükleme Hizi MPa/sn 0.050
Yükleme Hizi kN/sn 0.375
Alan (mm2) 7500
Hacim (cm3) 16875
0.000
Anlik Hiz MPa/s

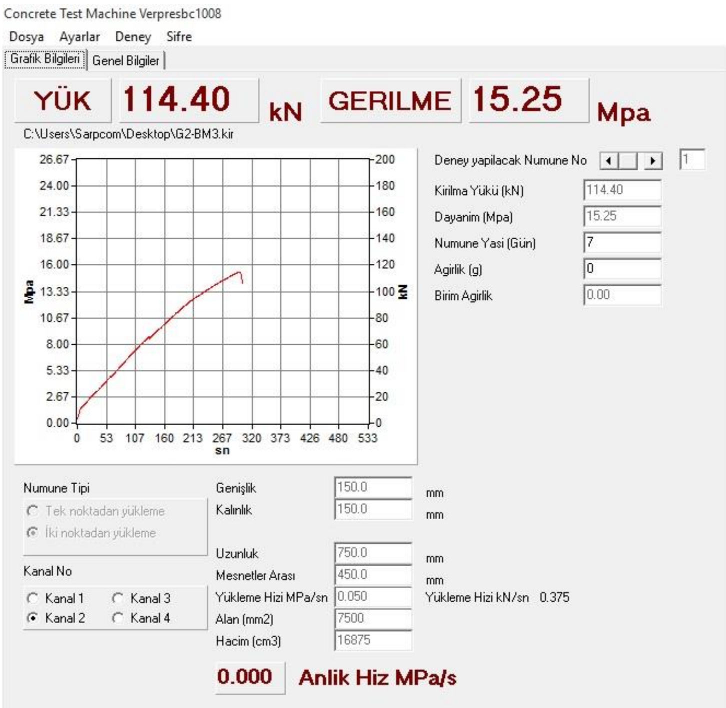

Concrete Test Machine Verpresbc1008
Dosya Ayarlar Deney Sifre
Grafik Bilgileri
Genel Bilgiler
YÜK
114.40
kN
GERILME
15.25
Mpa
C:\Users\Sarpcom\Desktop\G2-BM3.kir
Mpa
kN
sn
Deney yapilacak Numune No
Kirilma Yükü (kN) 114.40
Dayanim (Mpa) 15.25
Numune Yasi (Gün) 7
Agirlik (g) 0
Birim Agirlik 0.00
Numune Tipi
Tek noktadan yükleme
İki noktadan yükleme
Kanal No
Kanal 1
Kanal 2
Kanal 3
Kanal 4
Genişlik 150.0 mm
Kalınlık 150.0 mm
Uzunluk 750.0 mm
Mesnetler Arası 450.0 mm
Yükleme Hizi MPa/sn 0.050
Yükleme Hizi kN/sn 0.375
Alan (mm2) 7500
Hacim (cm3) 16875
0.000
Anlik Hiz MPa/s

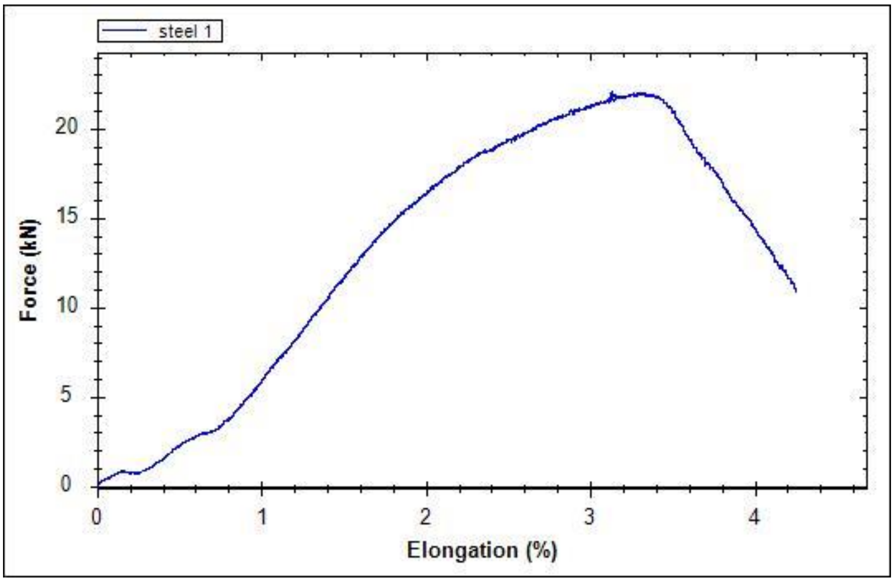

steel 1
Force (kN)
Elongation (%)

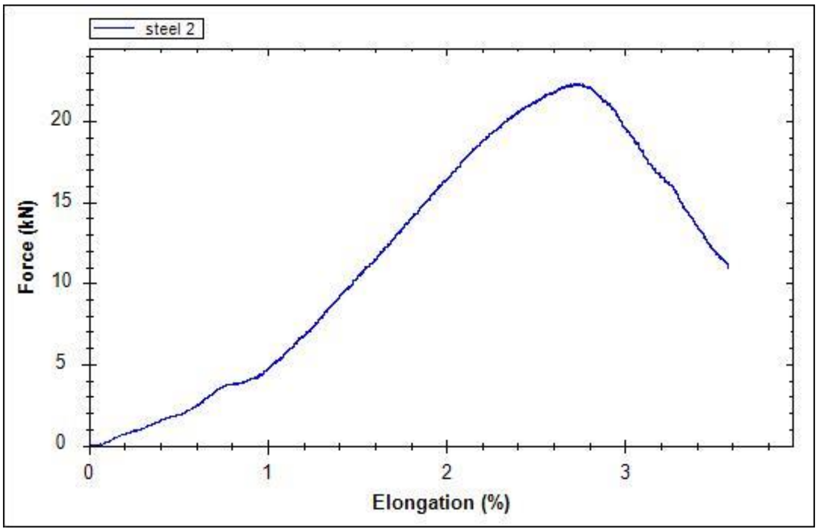
steel 2
Force (kN)
0
5
10
15
20
0
1
2
3
Elongation (%)

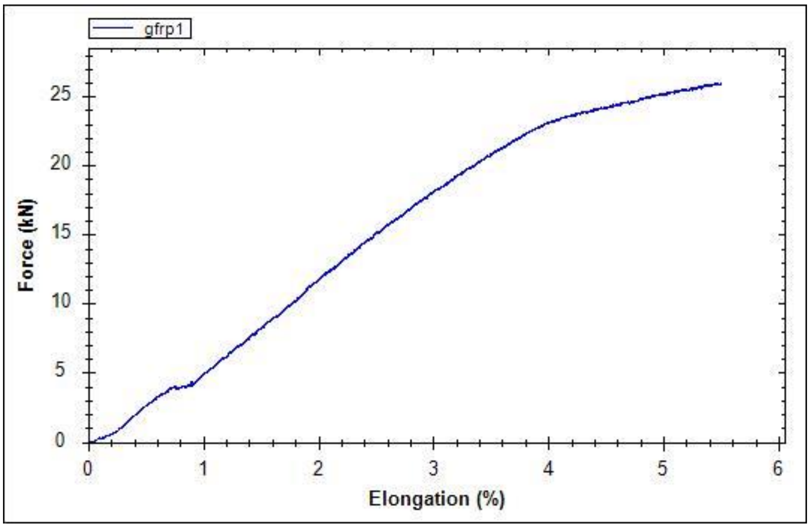
gfrp1
Force (kN)
0
5
10
15
20
25
0
1
2
3
4
5
6
Elongation (%)

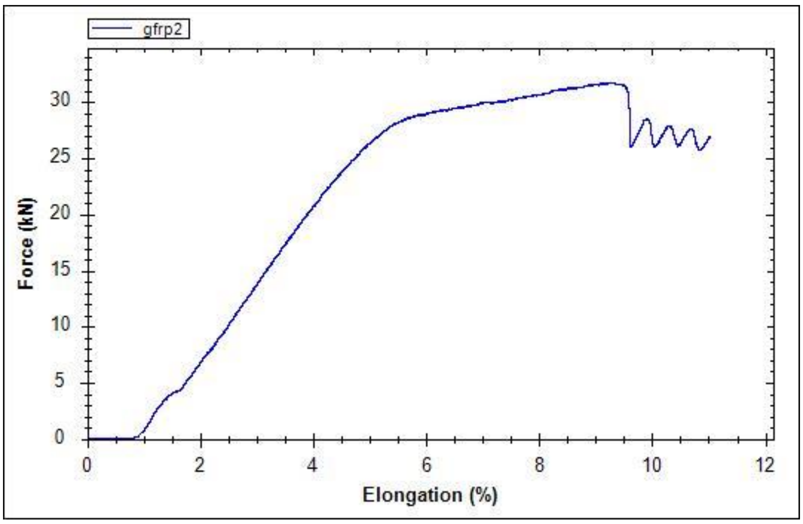
gfrp2
Force (kN)
0
5
10
15
20
25
30
0
2
4
6
8
10
12
Elongation (%)

Appendix 2

Stress strain relationship of concrete parameters

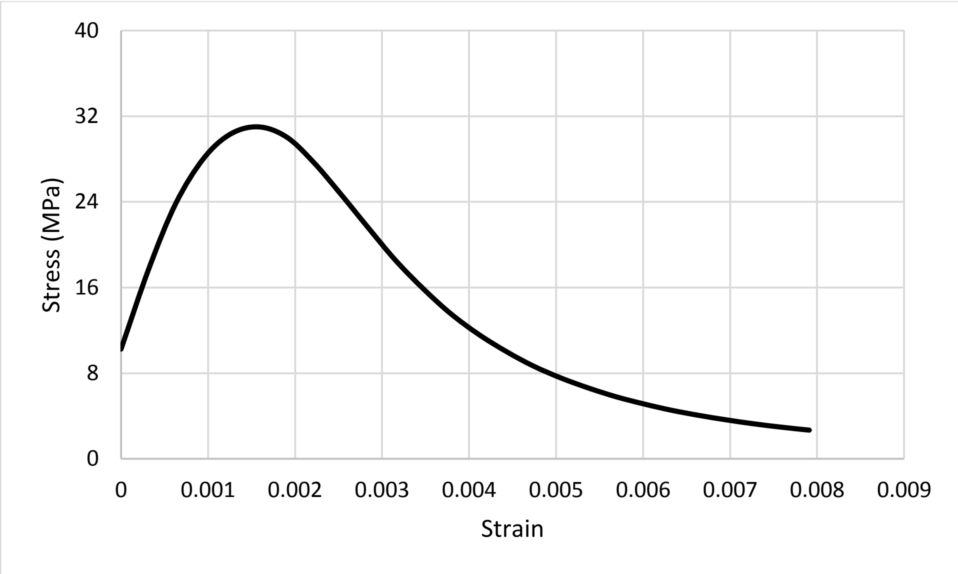

Figure A.2.1: Compression behaviour of concrete

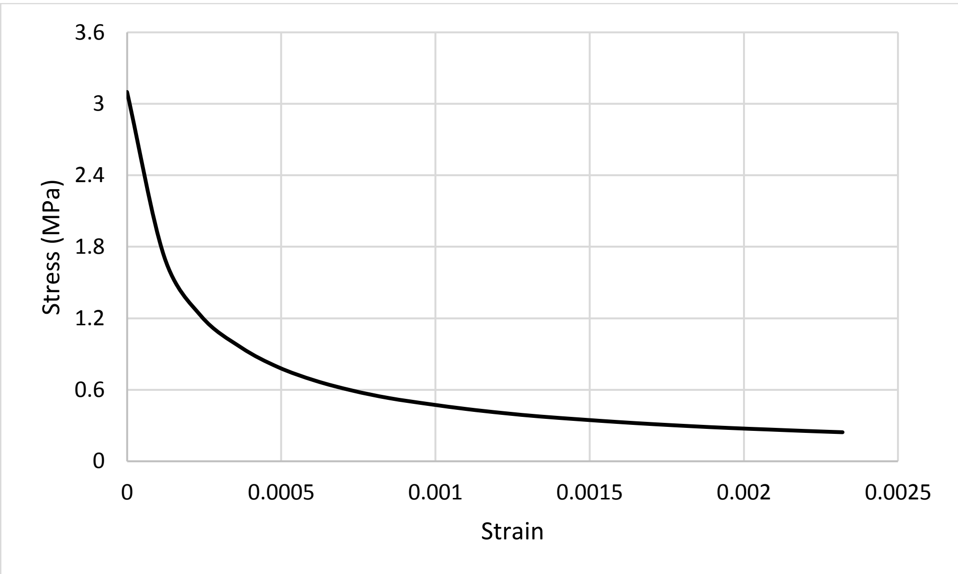

Figure A.2.2: Tension behaviour of concrete

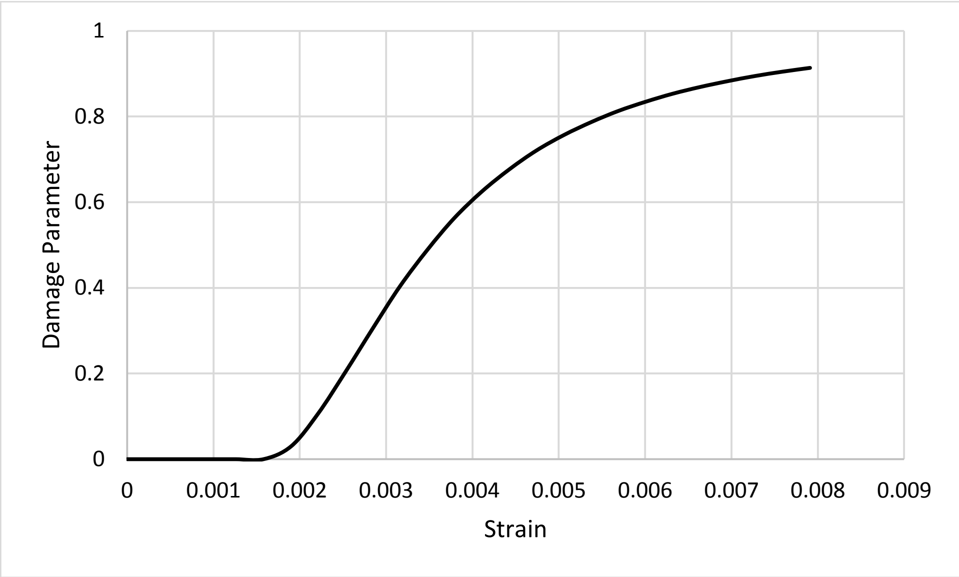

Figure A.2.3: Concrete compression damage

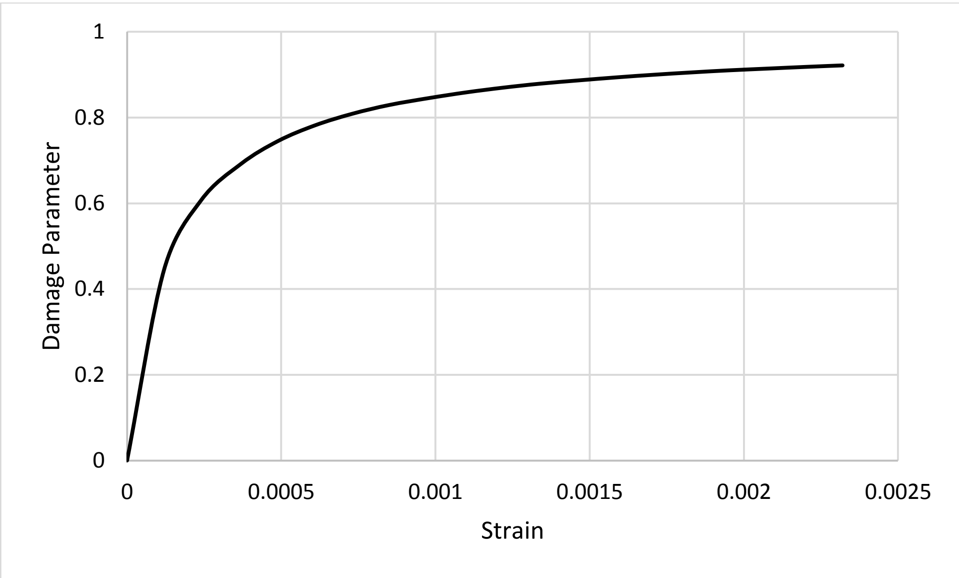

Figure A.2.4: Concrete tension damage

Appendix 3

Price list of Liana glass fibre reinforced polymer (GFRP) bar

ЛИАНА

Commercial Research and Production Association

Ural Reinforcing Company, Ltd.

(OOO«KNPO «Uralskaya Armiruischaya Compania» - in Russian)

De Jure Address: Cherneshevskogo 15b-149, 614039, Perm City, Russia
De Facto Address: Cherneshevskogo 15b-149, 614039, Perm City, Russia
tel./fax: +7 342 276 95 95
e-mail: uralsarmcompany@yandex.ru

Price List

Liana™ Non-Metallic Reinforcement

Diameter, mm	Liana™ GFNR	Liana™ BFNR HM
6	0.21 $	The price is defined individually according to order size
8	0.32 $	
10	0.46 $	
12	0.60 $	
14	0.81 $	

Prices are given for 1 running metre of composite reinforcement. The standard length is 12 runnin metres and also may vary according to individual requirements.